Doctoral Thesis

Development of Agglomeration-Flotation for Finely Ground Copper Sulfides

A dissertation submitted in partial fulfillment of the requirements for the degree of Doctorate in Engineering

by

VOTHY HORNN

Laboratory of Mineral Processing and Resources Recycling,
Division of Sustainable Resources Engineering,
Graduate School of Engineering,
Hokkaido University, Japan
September 2020

Abstract

Porphyry copper deposits (PCDs) are the main sources of copper (Cu), accounting for more than 60% of the annual production of Cu and are relatively low-grade, epigenetic, intrusion-related deposits that are commonly mined by open-pit methods. Despite their relatively low grades, PCDs have significant societal and economic impact due to their large size (up to billions of metric tons), long mine lives, and scale of mining operations. The ore containing chalcopyrite ($CuFeS_2$) in PCDs is generally processed by flotation to improve the Cu grade and remove the associated gangue minerals before smelting. In flotation, liberated Cu-bearing sulfide particles (e.g., chalcopyrite) are recovered via their selective attachment to air bubbles by changing their surface properties from hydrophilic to hydrophobic using collectors (e.g., xanthate). To maintain the high efficiency of Cu sulfide flotation, the ores have to be adequately ground to liberate Cu-bearing sulfide minerals from the unwanted gangue minerals. Recently, easily exploitable PCDs are very limited, which makes it unavoidable for mining industries to develop and exploit complex ore bodies with low grade and fine grain size. The ores containing fine-sized mineral grains require extensive grinding to achieve sufficient liberation that leads to the generation of large fractions of fines.

Despite its importance and widespread application in mineral processing, flotation still suffers from drawbacks, primary of which is its low recovery efficiency for fine particles (less than 10 μm for sulfides). In the flotation of fine particles, collisions between rising bubbles and the particles become poor because of the small mass and low momentum of the particles. Because of this, fine particles do not attach to bubbles, leading to substantial losses of recoverable minerals.

In this study, a new hybrid process of oil agglomeration—a method to increase the apparent size of particles—and flotation is proposed to reduce the substantial loss of fine chalcopyrite. Important factors like agitation strength, reagent dosage and stability of oil-water emulsion that affect the agglomeration-flotation process were investigated. In addition, a mathematical model for the flotation kinetics of agglomerated particles, which will be useful in designing and optimizing the agglomeration-flotation process, was developed. From the findings, a new process combining agglomeration and flotation using emulsified oil stabilized by emulsifiers that is cost-effective and could be easily integrated into conventional flotation circuits is proposed.

Chapter 1 describes the statement of the problem and the objectives of this study.

Chapter 2 reviews previous works about techniques to improve the recovery of fine particles in flotation, including micro-bubble flotation, column flotation, shear flocculation, carrier flotation, oil agglomeration, and polymer flocculation.

In Chapter 3, flotation experiments of finely ground chalcopyrite were carried out with and without oil-agglomeration as pretreatment and the kinetic data (time-recovery curves) were compared with the conventional first-order kinetic model for flotation. Agglomeration using kerosene as bridging

liquid improved Cu recovery from 45 to 90% because the apparent size of particles after agglomeration increased from 4 to 10 μm. Without agglomeration, time-recovery curves determined by the experiments fitted well with the model calculations, but there were significant deviations between experimental results and model calculations for the agglomerated particles; that is, experimental flotation recoveries were much higher than those calculated by the model. The conventional first-order kinetic model does not consider particle size changes during flotation while the experimental results suggested that the size of agglomerates increased in the flotation cell. A new flotation model that combines agglomeration during flotation was proposed, which could predict the time-recovery of agglomeration-flotation.

In Chapter 4, the effects of agitation strength during agglomeration, kerosene dosage and potassium amyl xanthate (KAX) dosage on flotation were investigated. With increasing agitation strength, KAX and kerosene dosages, Cu recovery was further improved. High agitation strength produces smaller oil droplets and more stable oil-water emulsion which resulted in high Cu recovery.

In Chapter 5, a new agglomeration-flotation process using emulsified oil stabilized by emulsifiers is proposed. Although high agitation during agglomeration improved Cu recovery, it required high energy, which makes the process costly. Moreover, emulsified oil should be added to agglomeration vessel immediately because emulsified oil is inherently unstable. In a commercial plant, stability of emulsified oil is important to keep size of “droplets” minute for oil agglomeration. Because of this, the effects of emulsifiers on the size of droplets in emulsified oil were investigated. When emulsifiers were added, oil droplet size in emulsified oil became small and stable. The small size and stability of emulsified oil made the agglomerates bigger, allowing for high Cu recovery in flotation to be achieved. When emulsified oil with emulsifiers was used, special equipment with higher agitation strength during agglomeration is unnecessary, and thus, the process could be easily integrated into existing flotation circuits.

Chapter 6 summarized the important findings of this dissertation and its implications.

Contents

CHAPTER 1: GENERAL INTRODUCTION

1.1 Background

Copper is an important base metal and the main sources of copper are from the porphyry copper deposits (PCDs). Porphyry copper deposits are the most important source of copper worldwide, accounting for more than 60% of the annual production of copper and they constitute about 65% of known copper ore resources (John et al., 2010). The porphyry ore deposits are commonly categorized as multi-zone deposits, composed of a primary sulfide ore at depth, a secondary enrichment zone, and a naturally weathered (oxidized) zone where all of the copper minerals have been oxidized (Bartlett, 1992). Fig. 1.1 shows a typical mining operation and copper extraction done in the porphyry copper deposits. In porphyry copper deposits, both oxide and sulfide copper minerals are usually mined by open-pit method (Robinson and Menzie, 2012). Copper oxides are often processed in a hydrometallurgical treatment, heap-leaching/solvent-extraction/electrowinning, to produce electric copper as a final product. Copper sulfides are treated in a mineral processing plant at mine site: run-of-mine ores are crushed and ground to liberate mineral grains and the ground ores are treated by flotation to remove gangue minerals such as quartz and to produce copper sulfide concentrate. The copper sulfide concentrate is then sent to smelters and copper is produced through a pyrometallurgical treatment.

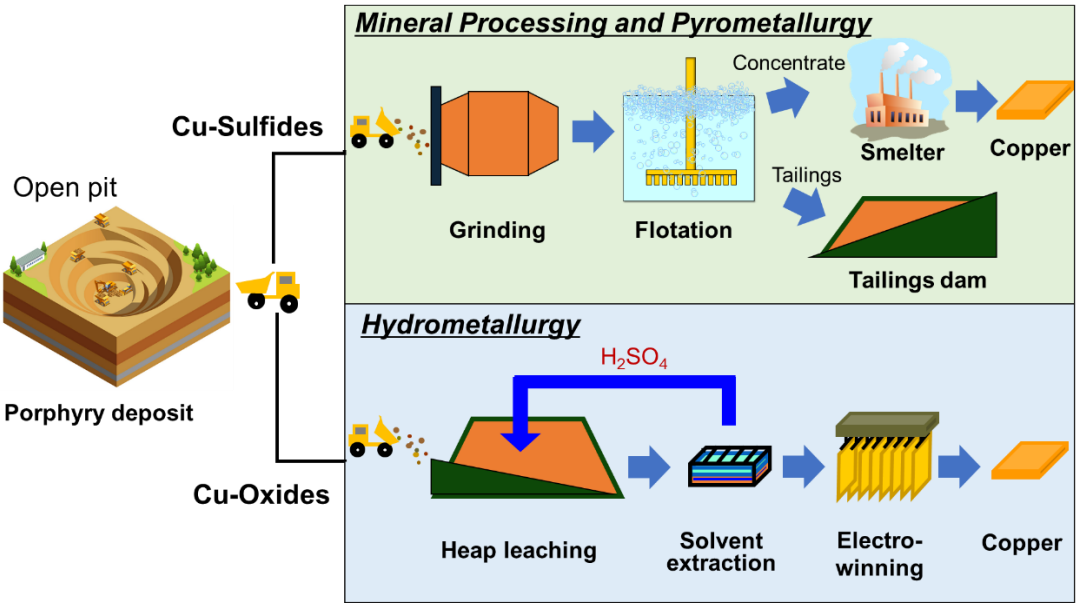

Fig. 1.1. Typical processes of copper production worldwide

In the flotation process, desired mineral particles are selectively attached onto air bubbles by changing the surface properties of the particles (from hydrophilic to hydrophobic) (Crozier, 1992). To concentrate the valuable minerals from these Cu sulfides ore in flotation, the ores have to be ground

to liberate valuable minerals from the unwanted gangue minerals. The presence of fine particles in flotation circuits is largely the result of excessive grinding, performed to attain higher degrees of mineral liberation. Recently, easily exploitable PCDs are very limited, which makes it unavoidable that mining industries must develop complicated ore deposits with low grade and fine grain size as shown in Fig. 1.2. The ores containing fine grain size require extensive grinding to achieve liberation, something that leads to the generation of large fractions of fines.

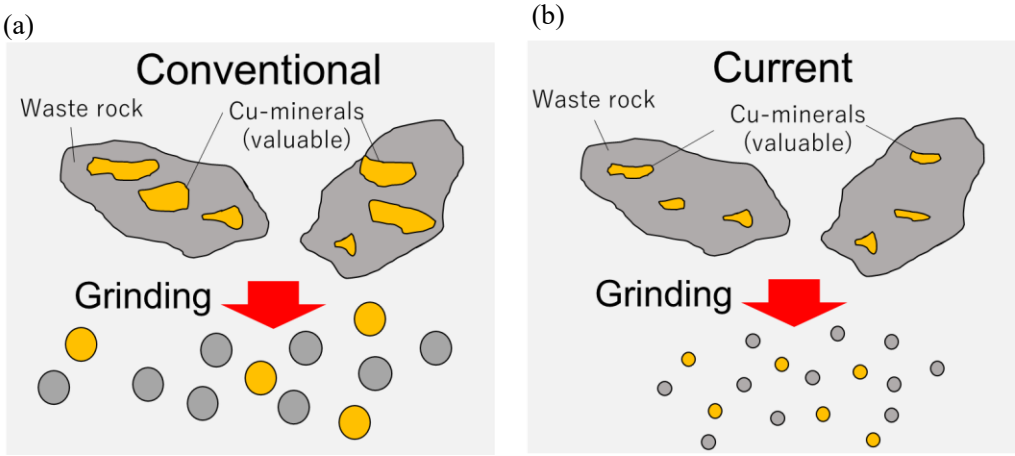

Fig. 1.2. Grinding and liberation of valuable minerals from the unwanted minerals particle; (a) Conventional liberation of valuable minerals of big grain size, and (b) liberation of more complicated ores (i.e. smaller grain size of valuable minerals).

Despite its importance and widespread application in mineral processing, flotation still suffers from drawbacks, the primary of which is the low efficiency in the recovery of fine particles (< 5 μm). Fine particles are difficult to process by flotation because of their low collision efficiency (attachment probability) with bubbles especially in widely used mechanical-type flotation apparatus. Flotation is also conducted in a dynamic environment where there are a great many interconnected factors playing difficult to determine roles in the process (King, 2000). For instance, mineral particles have to remain in contact with air bubbles for durations long enough to enable attachment in order for them to be floated (Nguyen-Van, 1994; Tortorelli et al., 1997).

Many studies have suggested ways to get around this problem of poor fine particle recovery in flotation using two approaches: (1) bubble size reduction, and (2) particle agglomeration.

1.2 Objective of the research

This research aims to develop agglomeration technology for improving the fine copper sulfides recovery in the flotation circuits.

1.3 Outline of the dissertation

This dissertation is composed of six chapters. The key contents of each chapter are outlined as follows:

Chapter 1 describe the statement of the problem, background of fine particle problems in flotation and objectives of this study.

Chapter 2 reviewed technologies to improve fine recovery in flotation, including microbubble flotation, column flotation, shear flocculation, carrier flotation polymer flocculation, and oil agglomeration.

In chapter 3, flotation experiments of finely ground chalcopyrite are carried out with and without oil agglomeration as pretreatment and the kinetic data (time-recovery curves) are compared with the conventional first-order kinetic model for flotation. A mathematical kinetic model for the flotation of agglomerate would be useful to design and optimize the agglomeration-flotation process, but no generally applicable model has been established yet. A new approach to estimate the recovery rate of flotation of agglomerate will be proposed.

In chapter 4, the effects of agitation strength during agglomeration, kerosene dosage and potassium amyl xanthate (KAX) dosage on the flotation are investigated. Agglomeration-flotation of a mixture containing chalcopyrite and quartz with 1:1 ratio (w/w) are also investigated.

In chapter 5, agglomeration-flotation using emulsified oil stabilized by emulsifiers is studied. The effects of emulsifiers on emulsified oil, agglomeration, and flotation are investigated.

Chapter 6 summarize the most important findings of this dissertation.

References

Bartlett, R. W. (1992). Percolation leaching oxidized and secondary sulfide copper minerals. In *Solution mining: leaching and fluid recovery of materials*, Gordon and Breach Science, Publishers, Philadelphia, 76-107.

Crozier, R. D. (1992). Flotation fundementals. In *Flotation: Theory, Reagents and Ore Testing*. Pergamon, p.5.

John, D.A., Ayuso, R.A., Barton, M.D., Blakely, R.J., Bodnar, R.J., Dilles, J.H., Gray, Floyd, Graybeal, F.T., Mars, J.C., McPhee, D.K., Seal, R.R., Taylor, R.D., and Vikre, P.G. (2010). Porphyry Copper Deposit Model, chap. B of Mineral deposit models for resource assessment: U.S. Geological Survey Scientific Investigations Report 2010–5070–B, p. 169.

Nguyen-Van, A. (1994). The Collision between Fine Particles and Single Air Bubbles in Flotation. *Journal of Colloid and Interface Science*, *162*(1), 123–128. https://doi.org/10.1006/jcis.1994.1016

Robinson, G. R. Jr., and Menzie, W. D. (2012). *Economic filters for evaluating porphyry copper deposit resource assessments using grade-tonnage deposit models, with examples from the U.S. Geological Survey global mineral resource assessment* (Global Mineral Resource Assessment No. 2010–5090; Scientific Investigations Report). U.S. Geological Survey. 10.3133/sir20105090H

Tortorelli, J. P., Craven, J. W., Toguri, J. M., Dobby, G. S., and Agar, G. E. (1997). The effect of external gas/slurry contact on the flotation of fine particles. *Minerals Engineering*, *10*(10), 1127–1138. https://doi.org/10.1016/S0892-6875(97)00099-X

CHAPTER 2: LITERATURE REVIEWS

2.1 Introduction

Flotation is widely used for the treatment of fine-sized sulfide minerals (<75 μm) (Napier-Munn and Wills, 2006). In this process, desired mineral particles are selectively attached onto air bubbles by changing the surface properties of the particles (from hydrophilic to hydrophobic) (Crozier, 1992). Despite its importance and widespread application in mineral processing, flotation still suffers from drawbacks, the primary of which is the low efficiency in the recovery of fine particles (<20μm) (Sivamohan, 1990; Trahar, 1981). The presence of fine particles in flotation circuits is largely the result of excessive grinding, performed to attain higher degrees of mineral liberation. Other factors like ore type and ore formation characteristics may also exacerbate this problem. Recently, this problem has increased in seriousness because of the need to exploit sulfide ore deposits with lower grades and more complex compositions. The types of ores here require extensive grinding to achieve liberation, something that leads to the generation of large fractions of fines (Bagster and McIlvenny, 1985). Fine particles are difficult to process by flotation because of their low collision efficiency (attachment probability) with bubbles especially in widely used mechanical-type flotation apparatus (Dai et al., 2000; Yoon, 2000). Flotation is also conducted in a very dynamic environment where there are a great many interconnected factors playing difficult to determine roles in the process (King,200). For instance, mineral particles have to remain in contact with air bubbles for durations long enough to enable attachment in order for them to be floated (Nguyen-Van, 1994; Tortorelli et al., 1997).

In flotation, desired mineral particles are recovered by selective attachment onto air bubbles and recovery rate (time-recovery ratio weight percentage) are mainly depends on the probability of particles attaching to bubbles (P). This probability of particles attaching to bubbles (P) in the flotation cell can be expressed by the following equations (Eq. (2.1)) (Yoon, 200):

$$P = P_c \times P_a \times (1 - P_d) \tag{2.1}$$

$$P_c = A\left(\frac{D_p}{D_b}\right)^n \tag{2.2}$$

where P_c, P_a, and P_d are the probabilities of collision, attachment, and detachment, respectively, D_p, and D_b are the particle and bubble diameters, respectively, and A and n (＞1) are empirical constants that depend on the flow regime. Based on Eq. (2.2), the probability of collision (P_C) is directly dependent on the ratio of the particle and bubble diameters. When the size of particles becomes very small ($D_p \ll D_b$), Pc (the probability of collision) is steeply decreased, this causes low P (the probability of particles attaching to bubbles) something which could explain the very low recovery rates of fine particles observed in mechanical-type flotation cells.

Many studies have suggested ways to get around the problem of poor fine particle recovery by increasing the bubble-particle collision efficiency using two approaches: (1) a reduction of bubble size,

and (2) increases in the relative particle size by particle agglomeration (Miettinen et al., 2010; S. Song et al., 2001). In this chapter, these approaches will be reviewed.

2.2 Bubble size reduction approaches

2.2.1 Conventional column flotation

In actual flotation circuits, several flotation cells are used in series to attain maximum recovery of the desired minerals. In its simplest configuration, a circuit is composed of a set of so-called rougher, cleaner, and scavenger cells. The rougher flotation cells are usually a mechanical-type and come first in the circuit with the primary purpose of maximizing recovery of the desired minerals. The tailings from these cells still contain valuable minerals and are fed to scavenger cells to minimize loss of valuable minerals in the final tailings. The froth from the rougher cells goes to regrinding to liberate the so-called middlings (unliberated particles containing desired- and gangue-minerals). The product of this process is then feed to the next group of cells, the cleaner cells. Cleaner cells are predominantly column-type flotation cells,and are designed to generate smaller bubbles than the mechanical-type units (Finch, 1995). The smaller bubbles improve recovery ratios and grades of products because the increase in Pc as described in Eq. (2.2). Moreover, column flotation has higher selectivity because of a thick froth zone and the use of wash water to minimize entrainment (Sivamohan, 1990). The froth from the cleaning stage becomes the concentrate while the tailings here are returned to the rougher cells for further processing. Although highly efficient, column flotation still suffers from major drawbacks like the need for quiescent operational conditions, structural problems arising from the tall columns that are required, and frequent blockage of spargers (Hacifazlioglu and Sutcu, 2007; Rodrigues and Rubio, 2007; Sivamohan, 1990; Yoon, 1993).

Column flotation uses different types of bubble generators/spargers produced by different manufacturers of flotation machinery. There are three types of spargers distinguished by the principle of producing the bubbles. One type uses a porous material like rubber or cloth into which air is pumped to produce the bubbles. This type which has been in use longest suffers from durability problems (wear and tear), pore blockage by particles, and difficulties of maintaining the optimum bubble size (Finch, 1995; Fuerstenau et al., 2007). Another type, the so-called jetting-type, operates by forcing a mixture of air and water at high pressures through a small circular orifice (Finch, 1995; Fuerstenau et al., 2007), here fine bubbles are produced because of instabilities along the jet surface (Finch, 1995). Some examples of this type are the U.S. Bureau of Mines bubble generators (U.S.B.M), Cominco (Finch, 1995), Jameson (Clayton et al., 1991), and the Eriez/CPT spargers (*CavTube Sparging | Eriez Flotation Division,* n.d.). Finally, there is another type which employs the shearing motion of a mixture of slurry and air generating fine bubbles by passing through a specially designed tube (M. C. Fuerstenau et al., 2007). Good examples of this type are the commercially available Microcel^{TM} (Yoon, 1993), in-line mixer (Xu et al., 1996) and the “motionless” mixer developed by Hirajima et al. (1998),

which was used in the Toyoha mine flotation circuit.

The bubble size produced by these types is difficult to control in the actual operation. (Re reported that laboratory scale studies have shown that an in-line mixer bubble generator, which is similar to the Microcel™, produces bubbles of up to 0.35 mm in diameter. Peycha et al. (2006) compared Microcel™ and jet-type spargers and concluded that the former produced smaller bubbles than the latter, and that this increased the recovery slightly. However, the mean diameter of the bubbles created by these two types is still relatively large (1-3 mm in diameter).

2.2.2 Microbubble column flotation

As described above, the reduction of bubble diameter to a few micrometers (microbubbles) is one possible approach to get around the problems associated with fine-particle flotation. Technically, a microbubble is defined as an air bubble with a diameter in the 1 to 100 μm range (Takahara, 2014). Microbubble flotation is mainly performed with column-type flotation cells because of microbubble stability problems in agitated flotation cells (Yoon, 1993). For example, this technique has been used in laboratory-scale experiments to recover copper, zinc and lead from a complex sulfide ore which required ultrafine grinding (<5 μm) to liberate the valuable minerals (Kusaka, 2014). There are several studies and devices where the generation of microbubbles is used to improve the collision efficiency in flotation cells, and these are detailed in Table1.

Despite its potential, microbubble flotation suffers from the following problems (Miettinen et al., 2010). First, longer residence times in the flotation circuit are required because of the slow rising speed of the tiny bubbles with the attached mineral particles. Second, the tiny bubbles may attach to all kinds of fine particles in the cell reducing the selectivity of the process.

Table 2.1. Microbubble flotation technologies

Name	Minerals studied	Process/effects	References
Electro-flotation	Chalcopyrite (Size: -20um; average -4.42μm)	-Bubble generation by electrolysis -Improved recovery by electrolytic oxygen	(Bhaskar Raju and Khangaonkar, 1982)
Charged microbubble/ colloid gas aphrons (CGAs) microbubble	CuO and SiO_2 Size: -10μm	-Grade of CuO improved from 59.1% to 81.8% -Recovery of CuO improved from 58.3% to 76.5%	(Waters et al., 2008)

Microbubble flotation	Pyrite, chalcopyrite galena, and sphalerite	-Microbubble flotation of ultrafine sulfide minerals	(Kusaka, 2014)
Microbubble flotation	Galena and sphalerite	-Collectorless microbubble flotation using sodium hydrosulfide	(Murao, 2014)
Nano-microbubble	Chalcopyrite -Fines (-38+14μm) -Ultrafine (5-14μm)	-Bubble size (D_{90}=100 μ m) generated by hydrodynamic cavitation -Improved recovery of fine and ultrafine particles (16-21%)	(Ahmadi et al., 2014)

2.3 Selective agglomeration approaches

As mentioned above, an alternative approach to improve collision efficiency of bubbles and fine particles during flotation is to increase the size of the mineral particles by agglomeration. Many studies have been conducted, and some technologies have been developed to improve the fines recovery using this approach. These techniques include shear flocculation, oil agglomeration, carrier flotation, and polymer flocculation. A brief description of these technologies is listed in Table 2.2 and a schematic diagram of the governing mechanisms involved is illustrated in Fig. 2.1.

Table. 2.2. Brief description of the methods and technologies to agglomerate fine particles

Methods	**Reagents and Material**	**Types of Interaction**
Shear flocculation	Surfactant	Hydrophobic interaction
Oil agglomeration	Oil, surfactant	Capillary forces
Carrier flocculation	Surfactant, Carrier material	Hetero coagulation
Polymer flocculation	Polymer, surfactant	Hydrophobic, chemical, hydroxyl functional group, electrostatic

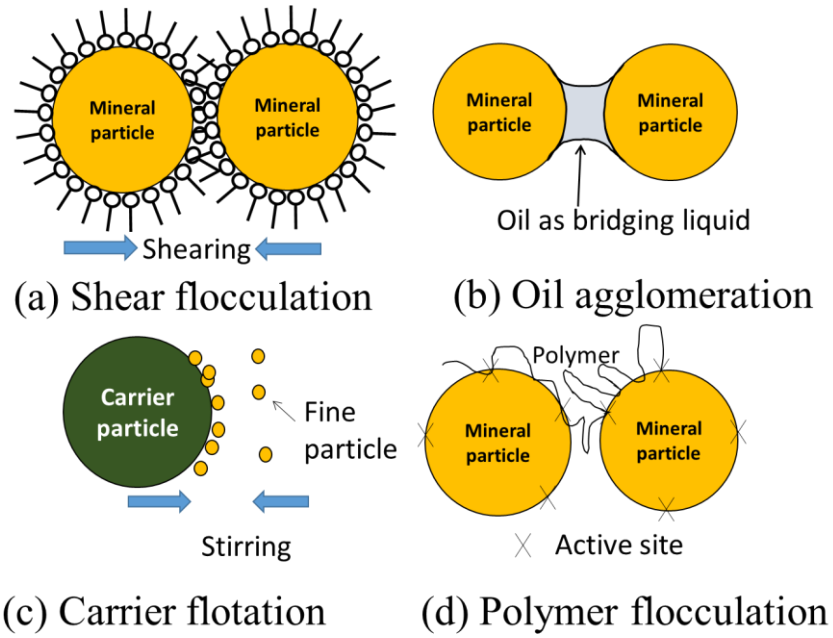

Fig. 2.1. Schematic representation of the four approaches in Table 2.1 to agglomerate fine particles: (a) Shear, (b) Oil, (c) Carrier, and (d) Polymer

2.3.1 Shear flocculation

Shear flocculation refers to the process by which hydrophobic fine minerals are aggregated under high shear conditions (usually by intense mixing) (Bilgen and Wills, 1991; Patil et al., 2001). It was initially proposed by Warren (1975) and described hydrophobic association as the reason behind the observed aggregation of fine scheelite in sodium oleate slurry after vigorous stirring. Warren (1975) suggested that the mechanism of the agglomeration occurs in via three steps: (1) thinning of the water interface surrounding the particles due to turbulent flow, (2) mutual attraction of the organic "tails" of surfactant components, and (3) entanglement of the organic "tails" see in Fig. 2.1(a). The final two steps were termed "hydrophobic association". Further, agglomeration was more effective using surfactants with longer "tails", and the aggregated products from this process were mechanically strong and at the same time hydrophobic, promoting the flotation. A later report, Warren (1992), modified this theory to include the effects of additional parameters like electrostatic and van der Waals forces as elucidated by the most recent and widely accepted theory of colloidal particle interactions, the so-called DLVO theory.

In DLVO theory (Derjaguin and Landau, 1993; Verway and Overbeek, 1948), named after Derjaguin, Landau, Verwey, and Overbeek, (shown in Fig. 2.2), the interactions between colloidal particles are explained based on two forces: (1) repulsive forces arising from electrostatic repulsion, and (2) van de Waals attraction. Depending on the conditions, total energy (summation of these two

forces) may create an energy barrier. However, DLVO theory is not sufficient to explain the phenomena occurring during shear flocculation, but it has been extended to include hydrophobic interactions (Bilgen and Wills, 1991, Xu and Yoon, 1989). There are also further suggestions for details of the hydrophobic interactions in Xu and Yoon (1989), Meyer et al. (2006), Attard (1989, 1996), Christenson and Claesson (1988), Claesson et al. (1986), and Israelachvili and Pashley (1984) but these will not be discussed further here. Warren (1992) estimated that the hydrophobic interaction energy is 2 to 10 times higher that of the van der Waals attractive energy. Although an additional attractive force is imparted by the hydrophobic interaction, this is still not sufficient to overcome the energy barrier imposed by the repulsive forces. This energy barrier could be overcome by the shearing forces due to vigorous stirring, which impart sufficient kinetic energy to enable direct contact between particles (Warren, 1975). Despite its promise, shear flocculation has found very limited application because of selectivity issues and the large energy inputs required.

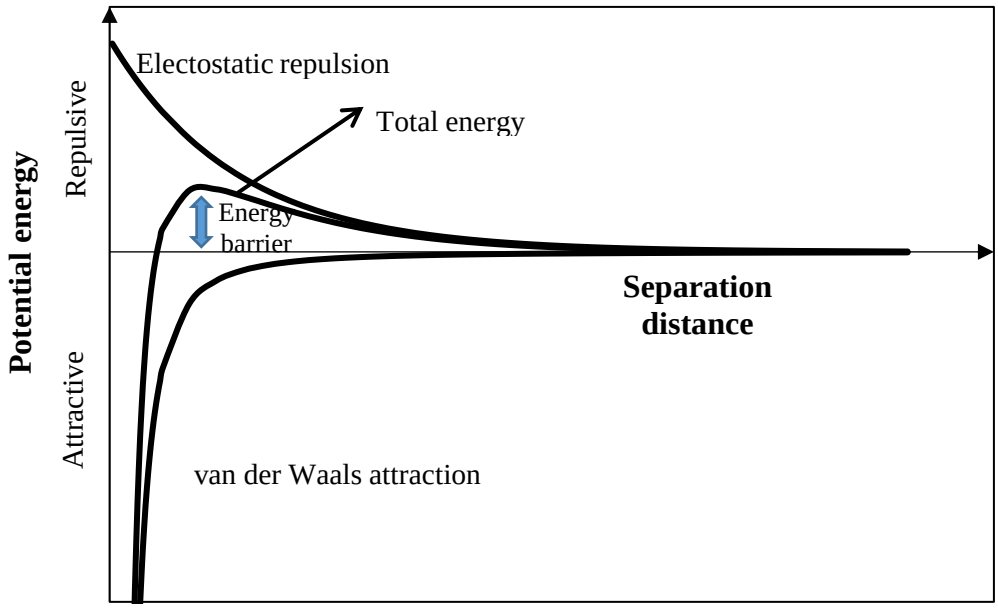

Fig. 2.2. Interaction of force acting on colloidal particles based on DLVO theory.

2.3.1.1 Controlling parameters

Two conditions have to be met for shear flocculation to occur: (1) the particles must be strongly charged, to facilitate their natural dispersion in the solution, and (2) the particles must be hydrophobic. These two factors are strongly influenced by other parameters such as pH, stirring speed, stirring time, amount and type of surfactants, and the kinetic energy provided by the stirring/ conditioning. For example, Dippenaar (1985) applied flocculation to galena and found that hexyl xanthate, which has a long hydrocarbon chain, produced better flocs than potassium ethyl xanthate which has a shorter

hydrocarbon chain (Song et al., 2001). The importance of the type of surfactant was also noted in the work of Warren (Warren, 1992) on cassiterite. Here it was reported that styryl phosphonic acid and benzyl arsenic acid did not induce shear flocculation, but that longer chained surfactants like sodium oleate and sulfosuccinamate were effective.

2.3.1.2 Case studies and applications to sulfide mineral flotation

Flotation tests after shear flocculation has also been reported by Song et al. (2001), with optimized conditions using pure galena or sphalerite (-20μm) and using the same parameters as in the shear flocculation and flotation of sulfide ore. High recovery rates of over 80% were achieved in the stirring speed of 900 rev/min and 700 rev/min for galena and sphalerite, respectively. At higher speeds, however, the recovery was poorer due to the rupture of the aggregates by the strong shearing energy/action.

Zhang and Qin (2014) examined fine marmatite (D_{50}= 4.24μm and D_{90}=-20 μm) flotation using ammonium butyl xanthate (KAX) and ammomonium dibutyl dithiophosphate (ADD). Addition of ADD and KBX increased the size of particles to 34 μm and 26μm, respectively, which improved the recovery to 20% higher than with conventional flotation.

2.3.2 Carrier flotation

In carrier flotation, larger size hydrophobic components (carrier) are used to capture the smaller valuable mineral particles and float them together (Ateşok et al., 2001; Chia and Somasundaran, 1983; Jorge Rubio and Hoberg, 1993). The collision efficiency of coarse and fine particles is better than that of fine-fine particles (shear flocculation), so the energy input with fine-large particles can be smaller than with fine-fine particles (Valderrama and Rubio, 1998; Warren, 1975a). For example, Fuerstenau et al. (1988) compared carrier flotation and shear flocculation-flotation and reported that recovery and grade of hematite of shear flocculation were higher carrier flotation. Carrier flotation was also applied to the first processing plant of the Mineral and Chemicals Phillip's Plants in Georgia to remove titanoferrous impurities from kaolinite using limestone (60µm) as the carrier. The two requirements for this process to occur, according to Subrahmanya and Frossberge (1990), are: (a) size differences of particles, and (b) mixing speed. Rabio and Hoberg (1993) reported carrier flotation with several minerals including oxide minerals such as apatite and quartz. They used polypropylene spheres as the carrier and pretreated it with emulsified oleic acid. The optimum conditions there were stirring conditions of 1500 rpm for 3 min and a size ratio of 4:1.

2.3.3 Polymer flocculation

Polymer flocculation is a process by which aggregation of fine mineral particles is achieved through a bridging effect of flocculants (Mathur et al., 2000). First flocculant interacts with mineral particles and then flocculation occurs through entanglement. Flocculants and fine particles generally interact

via hydrophobic interactions and/or chemical bonding (hydroxyl functional group bonding) (Mathur et al., 2000; Sivamohan, 1990; Somasundaran et al., 1996). An important parameter for flocculant adsorption selectivity is the solution pH because the net surface charge of minerals changes with pH (Sresty and Somasundaran, 1980). In 1975, polymer flocculation was applied to fine iron oxide ore in the Tilden iron ore mine, USA where polymer starch was used as the flocculant (Weissenborn et al., 1995).

Despite the promise, commercially successful applications of polymer flocculation in mineral processing are limited because of the low selectivity (Forbes, 2011). The main reason for this limitation is that most flocculants have been designed with hydroxyl functional groups that react with any mineral containing oxygen (Acar and Somasundaran, 1989; Attia, 1977; Mitchell et al., 2005; Sivamohan, 1990; Somasundaran et al., 1996). For instance, Accar and Somasundaran (1989) studied the possibility of selective flocculation for separation of chalcopyrite and pentlandite mixtures using polyacrylamide and polyethylene but found low separation efficiency for chalcopyrite and attributed it to the activation of pentlandite by dissolved species. The recovery was improved when diphenylgaunidine, a complexing agent, was added along with the polymer because this reagent limited the interference from dissolved species.

2.3.3.1 Enhancement of polymer flocculation

Enhancement of polymer selectivity is possible by adding dispersant, activators (Attia and Yostry, 1992) and site blocking agents (Mathur et al., 2000). When site blocking agents (SBA), for example, are used these could minimize hetero-coagulation and non-specific adsorption because they are more energetic than selective depressant (Mathur et al., 2000).

2.3.3.2 Cases study on sulfide mineral

Mandre and Panigrashi (1997) use the synthetized polymer xanthate (cellulose polymer) as flocculant when treating fine complex sulfides (size:57% is -13μm). They obtained very good recoveries, but low grades (3.3% and 10.6% for lead and zinc, respectively) suggesting that the flocculant used was non-selective.

2.3.4 Oil agglomeration

Oil agglomeration uses oil to aggregate minerals (Bensley et al., 1977; Wu et al., 2005). It is a process in which oil is used as connecting reagent/bridging liquid to bind the fine mineral particles through hydrophobic interactions under moderate to high shear conditions (Fig. 2.1b), which improve floatability by increasing the size of particles in the column (Jiangang et al., 2012). The agglomeration in this technique is attributed to capillary interfacial forces (Aktaş, 2002).

Oil agglomeration has been mostly studied in coal cleaning due to the high hydrophobicity of coal that allows easy agglomeration (Mehrotra et al., 1983). Some of the limiting factors of this technique in industrial scale operation are that it requires large amounts of oil and high energy inputs

(Bensley et al., 1977).

2.3.4.1 Controlling parameters

Type and dosage of oil, stirring speed, hydrophobicity of the minerals involved are all important parameters in promoting oil agglomeration (Aktaş, 2002; Alonso et al., 1999; Bos and Quast, 2000; Slaghuis and Ferreira, 1987; Wheelock et al., 1994). Oil is an expensive commodity, so to improve the economic viability of this process, the large amounts of oil required by this technique need to be reduced. Because of this, oil-water emulsification has also been introduced (Bensley et al., 1977). Emulsification decreases the size of oil droplets and increases their surface area (Sahinoglu and Uslu, 2013), which allows oil to fill the spaces created between mineral particles (van Netten et al., 2014).

2.3.4.2 Case studies on sulfide minerals

House and Veal (1989) showed that oil agglomeration (up to 100 kg/ton of ore) allows very selective recovery of fine chalcopyrite (D_{80}=23 μm) and sphalerite (D_{80}=23μm) in a mixture of sand, pyrite. This technique has also been applied to improve the recovery of fine sulfides (copper/molybdenite sulfide-type) (Rubio et al., 2007). In this study, diesel fuel (> 60g/ton) improved the recovery of fine (-37+5μm) and ultrafine (-5μm) sulfide particles by up to 4 and 5 %, respectively, compared to conventional flotation.

2.4 Summary

All of these techniques have their own benefits and drawbacks, but from the perspective of economics, oil-agglomeration is the most promising because oil is relatively inexpensive, the process could be easily integrated into existing flotation circuits, and the technique could effectively improve the recovery of fines. In this study, agglomeration-flotation of finely ground chalcopyrite was investigated.

References

Acar, S., and Somasundaran, P. (1989). Flocculation of sulfides and the role of a complexing agent in it. *International Journal of Mineral Processing*, *27*(1), 111–123. https://doi.org/10.1016/0301-7516(89)90009-4

Ahmadi, R., Khodadadi, D. A., Abdollahy, M., and Fan, M. (2014). Nano-microbubble flotation of fine and ultrafine chalcopyrite particles. *International Journal of Mining Science and Technology*, *24*(4), 559–566. https://doi.org/10.1016/j.ijmst.2014.05.021

Aktaş, Z. (2002). Some factors affecting spherical oil agglomeration performance of coal fines. *International Journal of Mineral Processing*, *65*(3–4), 177–190. https://doi.org/10.1016/S0301-7516(01)00074-6

Alonso, M. I., Valdés, A. F., Martínez-Tarazona, R. M., and Garcia, A. B. (1999). Coal recovery from coal fines cleaning wastes by agglomeration with vegetable oils: Effects of oil type and concentration. *Fuel*, *78*(7), 753–759. https://doi.org/10.1016/S0016-2361(98)00218-X

Ateşok, G., Boylu, F., and Çelīk, M. S. (2001). Carrier flotation for desulfurization and deashing of difficult-to-float coals. *Minerals Engineering*, *14*(6), 661–670. https://doi.org/10.1016/S0892-6875(01)00058-9

Attard, P. (1989). Long-range attraction between hydrophobic surfaces. *The Journal of Physical Chemistry*, *93*(17), 6441–6444. https://doi.org/10.1021/j100354a032

Attard, P. (1996). Bridging Bubbles between Hydrophobic Surfaces. *Langmuir*, *12*(6), 1693–1695. https://doi.org/10.1021/la950866w

Attia, Y. A. (1977). Development of a selective flocculation process for a complex copper ore. *International Journal of Mineral Processing*, *4*(3), 209–225. https://doi.org/10.1016/0301-7516(77)90003-5

Attia, Yostry A. (1992). Flocculation. In *Colloid Chemistry in Mineral Processing* (pp. 277–308). Elsevier.

Bagster, D. F., and McIlvenny, J. D. (1985). Studies in the selective flocculation of hematite from gangue using high molecular weight polymers. Part 1: Chemical factors. *International Journal of Mineral Processing*, *14*(1), 1–20. https://doi.org/10.1016/0301-7516(85)90010-9

Bensley, C. N., Swanson, A. R., and Nicol, S. K. (1977). The effect of emulsification on the selective agglomeration of fine coal. *International Journal of Mineral Processing*, *4*(2), 173–184. https://doi.org/10.1016/0301-7516(77)90024-2

Bhaskar Raju, G., and Khangaonkar, P. R. (1982). Electro-flotation of chalcopyrite fines. *International Journal of Mineral Processing*, *9*(2), 133–143. https://doi.org/10.1016/0301-7516(82)90022-9

Bilgen, S., and Wills, B. A. (1991). Shear flocculation—A review. *Minerals Engineering*, *4*(3), 483–487. https://doi.org/10.1016/0892-6875(91)90148-O

Bos, J. L., and Quast, K. B. (2000). Effects of oils and lubricants on the flotation of copper sulphide minerals. *Minerals Engineering*, *13*(14–15), 1623–1627. https://doi.org/10.1016/S0892-6875(00)00145-X

CavTube Sparging | Eriez Flotation Division. (n.d.). Retrieved June 10, 2016, from https://www.eriezflotation.com/sparging/cavtube-sparging/

Chen, G., and Tao, D. (2005). An experimental study of stability of oil–water emulsion. *Fuel Processing Technology*, *86*(5), 499–508. https://doi.org/10.1016/j.fuproc.2004.03.010

Chia, Y. H., and Somasundaran, P. (1983). A theoretical approach to flocculation in carrier flotation for beneficiation of clay. *Colloids and Surfaces*, *8*(2), 187–202. https://doi.org/10.1016/0166-6622(83)80084-5

Christenson, H. K., and Claesson, P. M. (1988). Cavitation and the Interaction Between Macroscopic Hydrophobic Surfaces. *Science*, *239*(4838), 390–392. https://doi.org/10.1126/science.239.4838.390

Claesson, P. M., Blom, C. E., Herder, P. C., and Ninham, B. W. (1986). Interactions between water—Stable hydrophobic Langmuir—Blodgett monolayers on mica. *Journal of Colloid and Interface Science*, *114*(1), 234–242. https://doi.org/10.1016/0021-9797(86)90257-2

Clayton, R., Jameson, G. J., and Manlapig, E. V. (1991). The development and application of the Jameson cell. *Minerals Engineering*, *4*(7), 925–933.

Crozier, R. D. (1992). Flotation fundementals. In *Flotation: Theory, Reagents and Ore Testing* (p. 5). Pergamon.

Dai, Z., Fornasiero, D., and Ralston, J. (2000). Particle–bubble collision models—A review. *Advances in Colloid and Interface Science*, *85*(2–3), 231–256. https://doi.org/10.1016/S0001-8686(99)00030-5

Derjaguin, B., and Landau, L. (1993). Theory of the stability of strongly charged lyophobic sols and of the adhesion of strongly charged particles in solutions of electrolytes. *Progress in Surface Science*, *43*(1–4), 30–59. https://doi.org/10.1016/0079-6816(93)90013-L

Dippenaar, A. (1985). *Mintek report* (No. M230; p. 19). Council for mineral technology, Randburg.

Feng, D., and Aldrich, C. (1999). Effect of particle size on flotation performance of complex sulphide ores. *Minerals Engineering*, *12*(7), 721–731. https://doi.org/10.1016/S0892-6875(99)00059-X

Finch, J. A. (1995). Column flotation: A selected review— part IV: Novel flotation devices. *Minerals Engineering*, *8*(6), 587–602. https://doi.org/10.1016/0892-6875(95)00023-J

Forbes, E. (2011). Shear, selective and temperature responsive flocculation: A comparison of fine particle flotation techniques. *International Journal of Mineral Processing*, *99*(1–4), 1–10. https://doi.org/10.1016/j.minpro.2011.02.001

Fuerstenau, D., Li, C., and Hanson, J. (1988). *Shear flocculation and carrier flotation of fine hematite*. 329.

Fuerstenau, M. C., Jameson, G. J., and Yoon, R.-H. (2007). Column Flotation. In *Froth Flotation: A Century of Innovation* (pp. 681–705). SME.

Grau, R. A., and Heiskanen, K. (2002). Visual technique for measuring bubble size in flotation machines. *Minerals Engineering*, *15*(7), 507–513. https://doi.org/10.1016/S0892-6875(02)00074-2

Grau, R. A., and Heiskanen, K. (2003). Gas dispersion measurements in a flotation cell. *Minerals Engineering*, *16*(11), 1081–1089. https://doi.org/10.1016/j.mineng.2003.06.007

Hacifazlioglu, H., and Sutcu, H. (2007). Optimization of some parameters in column flotation and a comparison of conventional cell and column cell in terms of flotation performance. *Journal of the Chinese Institute of Chemical Engineers*, *38*(3–4), 287–293. https://doi.org/10.1016/j.jcice.2007.03.006

Hirajima, T., Tomita, H., Takamori, T., and Tsunekawa, M. (1998). Development of high efficiency

flotation column. Comparision between new column and conventional column. *Journal of MMIJ*, *104*(1208), 754–757.

Hornn, V., Ito, M., Shimada, H., Joen, S., Park, I., Tabelin, C. B., and Hiroyoshi, N. (2019, 13-17). EARTH 2019. *Agglomeration Flotation of Finely Ground Chalcopyrite: Comparison of Model Calculation vs. Experimental Results*. EARTH 2019 THE 15th INTERNATIONAL SYMPOSIUM ON EAST ASIAN RESOURCES RECYCLING TECHNOLOGY, Korea.

Hornn, V., Ito, M., Shimada, H., Tabelin, C. B., Jeon, S., Park, I., and Hiroyoshi, N. (2020). Agglomeration-Flotation of Finely Ground Chalcopyrite and Quartz: Effects of Agitation Strength during Agglomeration Using Emulsified Oil on Chalcopyrite. *Minerals*, *10*(4), 380. https://doi.org/10.3390/min10040380

House, C. I., and Veal, C. J. (1989). Selective recovery of chalcopyrite by spherical agglomeration. *Minerals Engineering*, *2*(2), 171–184. https://doi.org/10.1016/0892-6875(89)90038-1

Israelachvili, J. N., and Pashley, R. M. (1984). Measurement of the hydrophobic interaction between two hydrophobic surfaces in aqueous electrolyte solutions. *Journal of Colloid and Interface Science*, *98*(2), 500–514. https://doi.org/10.1016/0021-9797(84)90177-2

Jiangang, F., Kaida, C., Hui, W., Chao, G., and Wei, L. (2012). Recovering molybdenite from ultrafine waste tailings by oil agglomerate flotation. *Minerals Engineering*, *39*, 133–139. https://doi.org/10.1016/j.mineng.2012.07.006

Johnson, C. P., Li, X., and Logan, B. E. (1996). Settling Velocities of Fractal Aggregates. *Environmental Science and Technology*, *30*(6), 1911–1918. https://doi.org/10.1021/es950604g

King, R. P. (2001a). Flotation (Section 9.2). In *Modeling and Simulation of Mineral Processing Systems* (pp. 312–313). Elsevier.

King, R. P. (2001b). *Modeling and Simulation of Mineral Processing Systems*. Elsevier.

Kusaka, E. (2014). Microbubble flotation of ultrafinely devided sulfide mineral. *The mining and materials processing institute of Japan*.

Latreille, B., and Paquin, P. (1990). Evaluation of Emulsion Stability by Centrifugation with Conductivity Measurements. *Journal of Food Science*, *55*(6), 1666–1668. https://doi.org/10.1111/j.1365-2621.1990.tb03595.x

Li, X., Hiroyoshi, N., Tabelin, C. B., Naruwa, K., Harada, C., and Ito, M. (2019). Suppressive effects of ferric-catecholate complexes on pyrite oxidation. *Chemosphere*, *214*, 70–78. https://doi.org/10.1016/j.chemosphere.2018.09.086

Mandre, N. R., and Panigrahi, D. (1997). Studies on selective flocculation of complex sulphides using cellulose xanthate. *International Journal of Mineral Processing*, *50*(3), 177–186. https://doi.org/10.1016/S0301-7516(97)00013-6

Mathur, S., Singh, P., and Moudgil, B. M. (2000). Advances in selective flocculation technology for

solid-solid separations. *International Journal of Mineral Processing*, *58*(1–4), 201–222. https://doi.org/10.1016/S0301-7516(99)00072-1

Mehrotra, V. P., Sastry, K. V. S., and Morey, B. W. (1983). Review of oil agglomeration techniques for processing of fine coals. *International Journal of Mineral Processing*, *11*(3), 175–201. https://doi.org/10.1016/0301-7516(83)90025-X

Meyer, E. E., Rosenberg, K. J., and Israelachvili, J. (2006). Recent progress in understanding hydrophobic interactions. *Proceedings of the National Academy of Sciences*, *103*(43), 15739–15746. https://doi.org/10.1073/pnas.0606422103

Miettinen, T., Ralston, J., and Fornasiero, D. (2010). The limits of fine particle flotation. *Minerals Engineering*, *23*(5), 420–437. https://doi.org/10.1016/j.mineng.2009.12.006

Mitchell, T. K., Nguyen, A. V., and Evans, G. M. (2005). Heterocoagulation of chalcopyrite and pyrite minerals in flotation separation. *Advances in Colloid and Interface Science*, *114–115*, 227–237. https://doi.org/10.1016/j.cis.2004.08.009

Mort, P. R. (2005). Scale-up of binder agglomeration processes. *Powder Technology*, *150*(2), 86–103. https://doi.org/10.1016/j.powtec.2004.11.025

Muganda, S., Zanin, M., and Grano, S. R. (2011). Influence of particle size and contact angle on the flotation of chalcopyrite in a laboratory batch flotation cell. *International Journal of Mineral Processing*, *98*(3), 150–162. https://doi.org/10.1016/j.minpro.2010.11.004

Murao, K. (2014). Fundemental study on the collectorless microbubble flotation using sadium hydrosulfide. *The mining and materials processing institute of Japan*.

Napier-Munn, T., and Wills, B. A. (2006). Flotation. In *Wills' mineral processing technology: An introduction to the practical aspects of ore treatment and mineral recovery*. Elsevier.

Nguyen-Van, A. (1994). The Collision between Fine Particles and Single Air Bubbles in Flotation. *Journal of Colloid and Interface Science*, *162*(1), 123–128. https://doi.org/10.1006/jcis.1994.1016

Park, I., Tabelin, C. B., Magaribuchi, K., Seno, K., Ito, M., and Hiroyoshi, N. (2018). Suppression of the release of arsenic from arsenopyrite by carrier-microencapsulation using Ti-catechol complex. *Journal of Hazardous Materials*, *344*, 322–332. https://doi.org/10.1016/j.jhazmat.2017.10.025

Patil, D. P., Andrews, J. R. G., and Uhlherr, P. H. T. (2001). Shear flocculation—Kinetics of floc coalescence and breakage. *International Journal of Mineral Processing*, *61*(3), 171–188. https://doi.org/10.1016/S0301-7516(00)00036-3

Polat, M., and Chander, S. (2000). First-order flotation kinetics models and methods for estimation of the true distribution of flotation rate constants. *International Journal of Mineral Processing*, *58*(1), 145–166. https://doi.org/10.1016/S0301-7516(99)00069-1

Pyecha, J., Lacouture, B., Sims, S., Hope, G., and Stradling, A. (2006). Evaluation of a MicrocelTM

sparger in the Red Dog column flotation cells. *Minerals Engineering*, *19*(6–8), 748–757. https://doi.org/10.1016/j.mineng.2005.09.044

Robinson, G. R. Jr., and Menzie, W. D. (2012). *Economic filters for evaluating porphyry copper deposit resource assessments using grade-tonnage deposit models, with examples from the U.S. Geological Survey global mineral resource assessment* (Global Mineral Resource Assessment No. 2010–5090; Scientific Investigations Report). U.S. Geological Survey. 10.3133/sir20105090H

Rodrigues, R. T., and Rubio, J. (2007). DAF–dissolved air flotation: Potential applications in the mining and mineral processing industry. *International Journal of Mineral Processing*, *82*(1), 1–13. https://doi.org/10.1016/j.minpro.2006.07.019

Rubio, J., Capponi, F., Rodrigues, R. T., and Matiolo, E. (2007). Enhanced flotation of sulfide fines using the emulsified oil extender technique. *International Journal of Mineral Processing*, *84*(1–4), 41–50. https://doi.org/10.1016/j.minpro.2007.04.002

Rubio, Jorge, and Hoberg, H. (1993). The process of separation of fine mineral particles by flotation with hydrophobic polymeric carrier. *International Journal of Mineral Processing*, *37*(1), 109–122. https://doi.org/10.1016/0301-7516(93)90008-X

Sahinoglu, E., and Uslu, T. (2013). Use of ultrasonic emulsification in oil agglomeration for coal cleaning. *Fuel*, *113*, 719–725. https://doi.org/10.1016/j.fuel.2013.06.046

Sivamohan, R. (1990). The problem of recovering very fine particles in mineral processing—A review. *International Journal of Mineral Processing*, *28*(3), 247–288. https://doi.org/10.1016/0301-7516(90)90046-2

Slaghuis, J. H., and Ferreira, L. C. (1987). Selective spherical agglomeration of coal. *Fuel*, *66*(10), 1427–1430. https://doi.org/10.1016/0016-2361(87)90191-8

Somasundaran, P., Das, K. K., and Yu, X. (1996). Selective flocculation. *Current Opinion in Colloid and Interface Science*, *1*(4), 530–534. https://doi.org/10.1016/S1359-0294(96)80123-3

Song, S., Lopez-Valdivieso, A., Reyes-Bahena, J. L., and Lara-Valenzuela, C. (2001). Floc flotation of galena and sphalerite fines. *Minerals Engineering*, *14*(1), 87–98. https://doi.org/10.1016/S0892-6875(00)00162-X

Song, Shaoxian, Lopez-Valdivieso, A., Reyes-Bahena, J. L., and Bermejo-Perez, H. I. (2001). Hydrophobic flocculation of sphalerite fines in aqueous suspensions induced by ethyl and amyl xanthates. *Colloids and Surfaces A: Physicochemical and Engineering Aspects*, *181*(1–3), 159–169. https://doi.org/10.1016/S0927-7757(00)00789-5

Sresty, G. C., and Somasundaran, P. (1980). Selective flocculation of synthetic mineral mixtures using modified polymers. *International Journal of Mineral Processing*, *6*(4), 303–320. https://doi.org/10.1016/0301-7516(80)90027-7

Stang, M., Karbstein, H., and Schubert, H. (1994). Adsorption kinetics of emulsifiers at oil—Water

interfaces and their effect on mechanical emulsification. *Chemical Engineering and Processing: Process Intensification*, *33*(5), 307–311. https://doi.org/10.1016/0255-2701(94)02000-0

Subrahmanyam, T. V., and Forssberg, K. S. E. (1990). Fine particles processing: Shear-flocculation and carrier flotation — a review. *International Journal of Mineral Processing*, *30*(3–4), 265–286. https://doi.org/10.1016/0301-7516(90)90019-U

Tabelin, C. B., Veerawattananun, S., Ito, M., Hiroyoshi, N., and Igarashi, T. (2017). Pyrite oxidation in the presence of hematite and alumina: I. Batch leaching experiments and kinetic modeling calculations. *Science of The Total Environment*, *580*, 687–698. https://doi.org/10.1016/j.scitotenv.2016.12.015

Takahara, T. (2014). Leading edge in fine bubble technology. *Journal of the Japan Institute of Energy*, *93*, 1022–1024.

Tortorelli, J. P., Craven, J. W., Toguri, J. M., Dobby, G. S., and Agar, G. E. (1997). The effect of external gas/slurry contact on the flotation of fine particles. *Minerals Engineering*, *10*(10), 1127–1138. https://doi.org/10.1016/S0892-6875(97)00099-X

Trahar, W. J. (1981). A rational interpretation of the role of particle size in flotation. *International Journal of Mineral Processing*, *8*(4), 289–327. https://doi.org/10.1016/0301-7516(81)90019-3

Trahar, W. J., and Warren, L. J. (1976). The flotability of very fine particles—A review. *International Journal of Mineral Processing*, *3*(2), 103–131.

Valderrama, L., and Rubio, J. (1998). High intensity conditioning and the carrier flotation of gold fine particles. *International Journal of Mineral Processing*, *52*(4), 273–285. https://doi.org/10.1016/S0301-7516(97)00068-9

van Netten, K., Moreno-Atanasio, R., and Galvin, K. P. (2014). Fine Particle Beneficiation through Selective Agglomeration with an Emulsion Binder. *Industrial and Engineering Chemistry Research*, *53*(40), 15747–15754. https://doi.org/10.1021/ie5027502

Verway, E., and Overbeek, J. T. G. (1948). Theory of Stability of Lyophobic ColloidsElsevier. *Amsterdam-New York*, 34.

Vinnett, L., Alvarez-Silva, M., Jaques, A., Hinojosa, F., and Yianatos, J. (2015). Batch flotation kinetics: Fractional calculus approach. *Minerals Engineering*, *77*, 167–171. https://doi.org/10.1016/j.mineng.2015.03.020

Warren, L. (1992). Shear flocculation. In *Colloid Chemistry in Mineral Processing* (Vol. 12, pp. 309–329). Elsevier Amsterdam.

Warren, L. J. (1975a). Shear-flocculation of ultrafine scheelite in sodium oleate solutions. *Journal of Colloid and Interface Science*, *50*(2), 307–318. https://doi.org/10.1016/0021-9797(75)90234-9

Warren, L. J. (1975b). Shear-flocculation of ultrafine scheelite in sodium oleate solutions. *Journal of Colloid and Interface Science*, *50*(2), 307–318. https://doi.org/10.1016/0021-9797(75)90234-9

Waters, K. E., Hadler, K., and Cilliers, J. J. (2008). The flotation of fine particles using charged microbubbles. *Minerals Engineering*, *21*(12–14), 918–923. https://doi.org/10.1016/j.mineng.2008.04.011

Weissenborn, P. K., Warren, L. J., and Dunn, J. G. (1995). Selective flocculation of ultrafine iron ore 2. Mechanism of selective flocculation. *Colloids and Surfaces A: Physicochemical and Engineering Aspects*, *99*(1), 29–43. https://doi.org/10.1016/0927-7757(95)03112-Q

Wheelock, T. D., Milana, G., and Vettor, A. (1994). Coal Utilization and the EnvironmentThe role of air in oil agglomeration of coal at a moderate shear rate. *Fuel*, *73*(7), 1103–1107. https://doi.org/10.1016/0016-2361(94)90245-3

Wu, X. Q., Monhemius, A. J., and Gochin, R. J. (2005). Quantitative assessment of hydrophobic agglomeration performance. *Minerals Engineering*, *18*(6), 567–573. https://doi.org/10.1016/j.mineng.2004.09.005

Xu, M., Quinn, P., and Stratton-Crawley, R. (1996). A feed-line aerated flotation column Part I: Batch and continuous test work. *Minerals Engineering*, *9*(5), 499–507. https://doi.org/10.1016/0892-6875(96)00038-6

Xu, Z., and Yoon, R.-H. (1989). The role of hydrophobic interactions in coagulation. *Journal of Colloid and Interface Science*, *132*(2), 532–541. https://doi.org/10.1016/0021-9797(89)90267-1

Yalcin, E., and Kelebek, S. (2011). Flotation kinetics of a pyritic gold ore. *International Journal of Mineral Processing*, *98*(1), 48–54. https://doi.org/10.1016/j.minpro.2010.10.005

Yoon, R. H. (2000). The role of hydrodynamic and surface forces in bubble–particle interaction. *International Journal of Mineral Processing*, *58*(1–4), 129–143. https://doi.org/10.1016/S0301-7516(99)00071-X

Yoon, R.H. (1993). Microbubble flotation. *Minerals Engineering*, *6*(6), 619–630. https://doi.org/10.1016/0892-6875(93)90116-5

Yoon, R.H., and Lutttrell, G. H. (1989). The Effect of Bubble Size on Fine Particle Flotation. *Mineral Processing and Extractive Metallurgy Review*, *5*(1–4), 101–122. https://doi.org/10.1080/08827508908952646

ZHANG, T., QIN, W., YANG, C., and HUANG, S. (2014). Floc flotation of marmatite fines in aqueous suspensions induced by butyl xanthate and ammonium dibutyl dithiophosphate. *Transactions of Nonferrous Metals Society of China*, *24*(5), 1578–1586. https://doi.org/10.1016/S1003-6326(14)63228-3

CHAPTER 3: KINETIC ANALYSIS FOR AGGLOMERATION-FLOTATION OF FINELY ROUND CHALCOPYRITE: COMPARISON OF FIRST ORDER KINETIC MODEL AND EXPERIMENTAL RESULTS

3.1 Introduction

Although previous studies as described in Chapter two have reported agglomeration-flotation as a promising technique to improve the floatability of finely ground mineral particles by increasing its apparent size, flotation model for agglomerated particles has not been established yet. A mathematical model for the flotation kinetics of agglomerated particles would be useful to design and optimize the agglomeration-flotation process. In this chapter, flotation experiments were carried out with and without oil-agglomeration, and the kinetic data obtained were analyzed using the conventional first-order kinetic model for flotation. Kinetic analysis of finely ground chalcopyrite during agglomeration-flotation was carried out to identify the factors and important parameters affecting the process for establishment of a flotation model for agglomerated mineral particles.

3.2 Materials and methods

3.2.1 Minerals and reagents

The chalcopyrite sample used in this study was obtained from Copper Queen Mine, Arizona, USA. The sample was crushed by a jaw crusher, ground in a ball mill, and sieved to less than 75 μm. The ground sample was then further purified by heavy liquid separation using sodium polytungstate ($Na_6(H_2W_{12}O_{40})$ solution (specific gravity of 3) to remove light gangue minerals like quartz. After heavy liquid separation, the sample was washed with 1 M HNO_3, rinsed thoroughly with deionized water, and dewatered with acetone under vacuum following the procedure employed by several authors to remove oxidation products on pyrite (Li et al., 2019; Park et al., 2018; Tabelin et al., 2017). The sample was analyzed by X-ray powder diffraction (XRD) (Multiplex, Rigaku Corporation, Japan) and X-ray fluorescence spectroscopy (XRF) (EDXL300, Rigaku Corporation, Japan), and the results showed that the sample is composed of 85% chalcopyrite with moderate to trace amounts of sphalerite, quartz and actinolite as gangue minerals. Before flotation or agglomeration-flotation, the washed sample was finely ground in a vibratory disc mill (RS100, Retsch Inc. Germany) to obtain samples having three different D_{50} (3, 10 and 22 μm measured in ethanol).

Potassium amyl xanthate (KAX) (Tokyo Chemical Industry Co., Ltd., Japan) was used as the surface modifier to improve the hydrophobicity of chalcopyrite before flotation and agglomeration. Kerosene (Wako Pure Chemical Industries, Ltd., Japan) was used as the “bridging” liquid of chalcopyrite particles, and methyl isobutyl carbinol (MIBC) (Tokyo Chemical Industry Co., Ltd., Japan) was used as the frother in flotation.

3.2.2 Flotation tests

Flotation tests of chalcopyrite samples were carried out using an agitator-type flotation machine (FT-1000, Heiko, Japan). A 20 g sample was suspended in 400 mL of distilled water (5% pulp density). A 200 g/t of KAX was added and stirred for 5 min in a flotation cell to improve the hydrophobicity of chalcopyrite. After conditioning with KAX, the frother (25 μL/L of MIBC) was added and the pulp was stirred for another 3 min and then flotation was carried out at a flow rate of 1 L/min followed by separate collection of froth products within the following time intervals: 0–0.5, 0.5–1, 1–2, 2–4, 4–7, and 7–10 min. All of the froth products and the final tailing were oven dried (105°C) for 24 hours, weighed and analyzed by XRF for the copper (Cu) recovery calculation.

3.2.3 Agglomeration-flotation tests

A 20 g sample was suspended in 400 mL of distilled water (5% pulp density) and stirred for 5 min in a flotation cell after adding 200 g/t of KAX to improve the hydrophobicity of chalcopyrite. After conditioning with KAX, the suspension was transferred to a high-speed mixer (SPB-600J, Cuisinart, USA) and 1.5 mL of kerosene-water emulsion (0.3 mL kerosene in 1.2 mL distilled water) was added, and then mixed for 30 min at a mixing speed of 15000 rpm to promote agglomeration. The agglomeration products were transferred to the flotation cell, and then flotation was carried out following the method outlined in the previous subsection.

3.2.4 Particle size distribution measurements

The particle size distributions of samples suspended in water were analyzed using laser diffraction sizer (Microtrac® MT3300SX, Nikkiso Co., Ltd., Japan). Accuracy of size measurement was confirmed by a preliminary experiment using different size fraction of ground chalcopyrite sample prepared by sieving. To determine the particle size of primary particles (i.e., un-agglomerated particles), the sample was suspended in ethanol and sonicated to disperse the particles prior to measurements by laser diffraction.

3.2.5 Bubble size distribution and bubble rising velocity measurements

Bubble size distribution measurements in a flotation cell were carried out based on the visual technique developed by Grau and Heiskanen (2002). The bubbles were drawn from the flotation cell into viewing chamber made of a single-crystal quartz “window” where undistorted pictures of bubbles could be captured using a high-speed (2000 frame per seconds) digital camera (HAS-L1, DITECT, Japan). The captured images were analyzed using an image analysis software, WinRoof v.5 (MITANI Corporation, Japan). Before the measurement, the pulp for flotation of chalcopyrite (5% pulp density) was filtered to removed solid residues and the filtered solution was mixed with kerosene (0.75 mL/L). This solution was transferred to the flotation cell and after conditioning with 25 μL/L MIBC, air was injected to

create bubbles for the measurements. The bubble rising velocities were also calculated from the change in position of the same bubble between 2 captured images from different frames.

3.2.6 Particle settling velocity measurements

For the measurement of particle settling velocity, agglomerated or un-agglomerated particle was suspended (0.1% pulp density) in a glass tube with a back-light source. Videos of settling particles were taken by a digital microscope (VHX-1000, Keyence Corporation, Japan) at 15 frames per second. The videos were then converted to images and the particle settling velocities were calculated based on settling distances of particles after 5 seconds.

3.3 The kinetic model for flotation

3.3.1 Probability of particle attachment by an air bubble (P)

During flotation, suspended particles will collide with a rising bubbles and some of these particles will attach to the bubble surface and will travel upwards with the bubble (King, 2001). The rate of collision of bubble-particles depends on many parameters such as the size of the bubble and the size of the particles, their relative velocities, and pulp density. The process of bubble-particle interaction during flotation is divided into three subprocesses, including collision, attachment, and detachment (Yoon, 2000). The probability (P) of a particle being collected by an air bubble in the pulp phase of a flotation cell can be given by

$$P = P_c P_a (1 - P_d) \tag{2.1}$$

where P_c is the probability of bubble-particle collision, P_a is the probability of attachment and P_d is the probability of detachment.

For fine particles, P_d can be negligibly small because of the low inertia, so Eq. (2.1) can be expressed as follows:

$$P = P_c P_a \tag{3.1}$$

P_c is determined by the hydrodynamics of the system, which is strongly affected by the particle size, bubble size and the turbulence of the system. P_a is also affected by the hydrodynamics but is largely a function of the surface chemistry involved. In this paper, $P_a = 1$ was used since chalcopyrite with KAX shows strong hydrophobic properties, in which case Eq. (3.1) becomes:

$$P = P_c \tag{3.2}$$

In this study, the probability of collision (P_c) model by Yoon and Luttrel (1989) was used (Eq. (3.3)).

$$P_c = [\frac{3}{2} + \frac{4Re_b{}^{0.72}}{15}](\frac{D_p}{D_b})^2 \tag{3.3}$$

where, Re_b is Reynold number of bubbles.

3.3.2 First-order kinetic model for flotation

Crushed samples have particle size distribution and these samples are treated by flotation. Recovery ratio of targeted mineral as froth with time, R, can be calculated by using a conventional first-order kinetic model. The recovery of particle having dimeter D_i, R_i as a function of time, t can be written as

$$\frac{dR_i}{dt} = k_i(1 - R_i) \tag{3.4}$$

$$R_i = 1 - e^{-k_i t} \tag{3.5}$$

where k_i is the kinetic constant. Recovery of target minerals having a particle size distribution η_i, R, can be written as

$$R = \sum \eta_i R_i = \sum \eta_i (1 - e^{-k_i t}) \tag{3.6}$$

In this study, measured size distributions of feed sample of flotation determined by laser diffraction were used for η_i, and the kinetic constant, k_i, was calculated as

$$k_i = n_b \times \frac{\pi}{4}\left(D_b + D_{pi}\right)^2 (v_b + v_i) \times P_{ci}\ P_{ai}\,(1 - P_{di}) \tag{3.7}$$

Number of bubbles per unit volume, n_b was calculated as

$$n_b = \frac{G_v \tau_b}{(\pi/6) D_b{}^3} \tag{3.8}$$

where, the specific aeration rate, G_v (m^3/s of air per m^3 cell volume) and average residence time of air bubble in the cell, $\tau_b[s]$ was calculated from $v_b[m/s]$, $\tau_b = v_b/L$. Rising velocity of bubble (v_b) was calculated based on the equation proposed by King (2001b) and L[m] is the water height in flotation cell. P_{ci}, P_{ai}, P_{di} are the probability of collision, attachment and detachment of a particle having diameter, D_{pi}, respectively.

As described above, P_{di} is negligible and P_{ai} is almost one and this Eq. (3.7) can be written as;

$$k_i = n_b \times \frac{\pi}{4}\left(D_b + D_{pi}\right)^2 (v_b + v_i) \times P_{ci} \tag{3.9}$$

The term, $\frac{\pi}{4}\left(D_b + D_{pi}\right)^2 (v_b + v_i)$, is the swept volume of a rising bubble (average diameter, D_b; rising velocity, v_b) against settling particles (diameter, D_{pi}; settling velocity, v_i) per unit time.

Particle settling velocity, v_i was calculated based on terminal settling velocity in the stoke region.

The bubble rising velocity, v_b is calculated by equation

$$v_b = \frac{D_{be}}{D_{bh}} \left(\frac{4(\rho_f - LLmax) g D_{be}}{3 C_D\, \rho_f}\right)^{\frac{1}{2}} \tag{3.10}$$

where LL_{max} is bubble load (LL_{max} = 0 is disregard in this calculation), D_{be} is effective bubble diameters, D_{bh} is bubble diameter projected on horizontal plan, ρ_f: Fluid density [kg/m^3], C_D is drag

coefficient. $\frac{D_{be}}{D_{bh}}$ is assumed to be 1 for small bubble less than 1 mm in diameter. As C_D is in the function of bubble Reynold number (R_{eb}), which also depends on bubble rising velocity, calculation approach of C_D was created by the relation between Reb and C_D is used.

The calculated value of P_{ci} (Eq. (3.3)) and k_i (Eq. (3.9)) as the function of particle diameter (D_{pi}) is shown in Fig. 3.1 and this value was used in the model calculation. Using Eq. (3.6), recovery of target minerals having a particle size distribution η_i, R can be calculated.

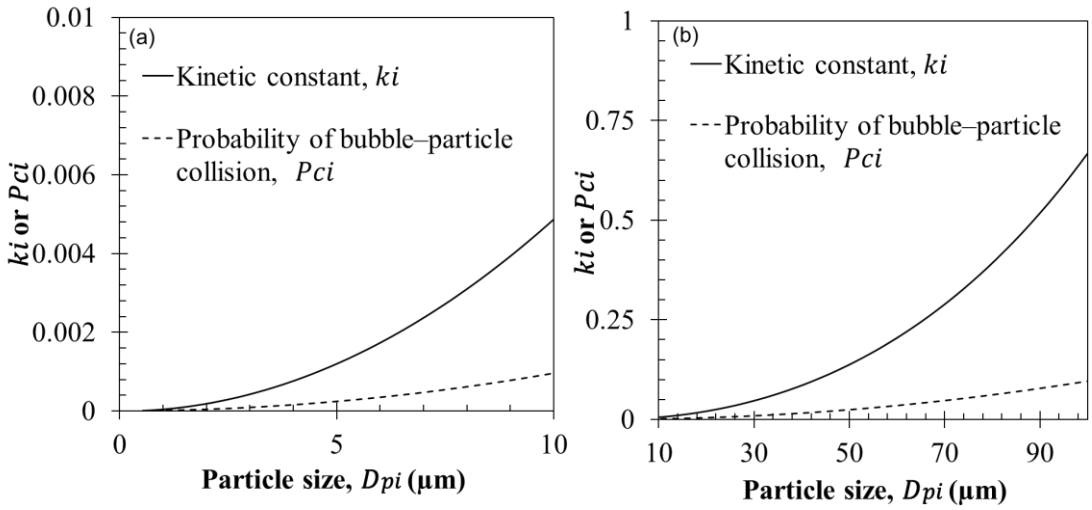

Fig. 3.1. Probability of bubble-particle collision(P_{ci}) and kinetic constant k_i of particle having diameter D_{pi}: (a) Particle diameter D_{pi} from 0-10 µm and (b) particle diameter D_{pi} from 10-100 µm. Particle terminal settling velocity (v_{Ti}) was calculated from stoke laws based on particle size (D_{pi}) and bubble rising velocity (v_b) was calculated using Eq. (3.10) with bubble diameters, Db= 0.9 mm.

3.4 Results and discussion

3.4.1 Flotation of un-agglomerated chalcopyrite

As mentioned in the previous section (3.3.1), the bubble-particle collision probability of fine particles is lower than that of larger particles. As a result, the recovery rate of smaller particles is slower than that of bigger particles. To confirm this particle size effect on flotation recovery, flotation experiments were conducted using ground chalcopyrite samples having different particle sizes (D_{50} = 3, 7 and 22 µm). As shown in Fig. 3.2, Cu recovery rate with time increased as particles became larger.

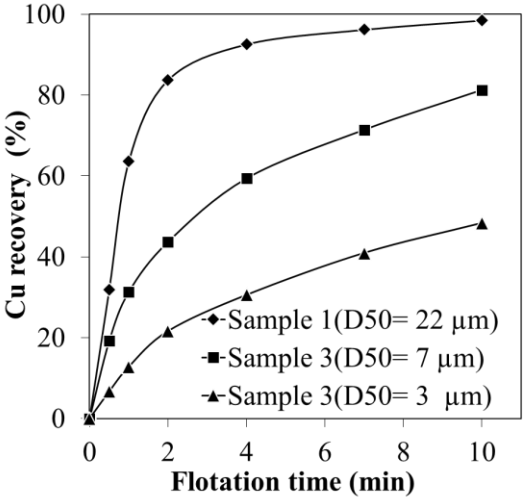

Fig. 3.2. Copper (Cu) recovery as a function of flotation time using three different size fractions of chalcopyrite: Sample 1(D_{50} = 22 μm), Sample 2 (D_{50} = 7 μm), and Sample 3 (D_{50} = 3 μm).

For model calculation, particle size distributions (volume-based) in ethanol (I) or water (II) were determined by laser diffraction as illustrated in Fig. 3.3. Plot (II) in Fig. 3.3 shows the size distribution curve of particles suspended in water after conditioning with KAX just before flotation. For comparison, the size distribution of primary particles (Plot (I) measured in ethanol) were also shown in this Fig. 3.3. By comparing Plots (I) and (II), it was apparent that flocculation occurred by simply conditioning fine chalcopyrite with KAX in the flotation cell. Flocculation occurs due to most likely to hydrophobic attraction of chalcopyrite particles and their increased hydrophobicity via adsorption of KAX. For the kinetic model calculations, the particle size distribution measured after conditioning with KAX (just before flotation) was used.

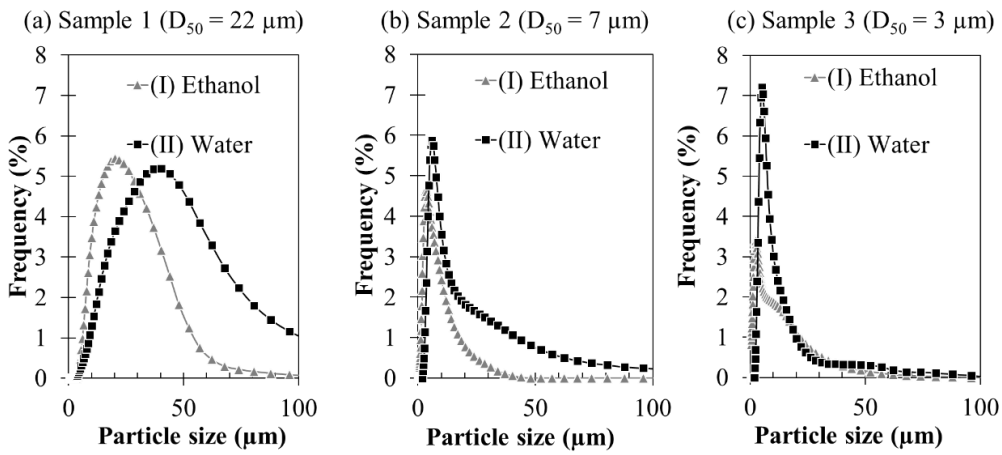

Fig. 3.3. Particle size distributions of the three samples ((a)Sample 1, (b)Sample 2, and (c)Sample 3) measured in ethanol (I) and water (II) after conditioning.

Fig. 3.4 shows the bubble size distribution (number-based) measured in the flotation cell. As shown in Fig. 3.4a, mode (peak) bubble size was around 0.9 mm, and the frequency was more than 30% at this bubble size. From the cumulative size distribution curve (Fig. 3.4b), it was observed that > 70% of bubbles were within the size range of 0.8 to 1.0 mm. Based on these results and to simplify the kinetic modeling calculations, the mode bubble size (D_b) of 0.9 mm was used.

The flotation recovery of Samples 1, 2 and 3 was calculated as a function of time using the first-order kinetic model described in section 3.3.2 (solid lines in Figs. 3.5a–c). For comparison, experimental results shown in Fig. 3.2 were also plotted in Fig. 3.5. The results showed that the first-order kinetic model fitted well with the experimental results, suggesting that this model is applicable for the flotation of un-agglomerated chalcopyrite samples. The similar results were also observed by several authors (Vinnett et al., 2015; Polat and Chander, 2000).

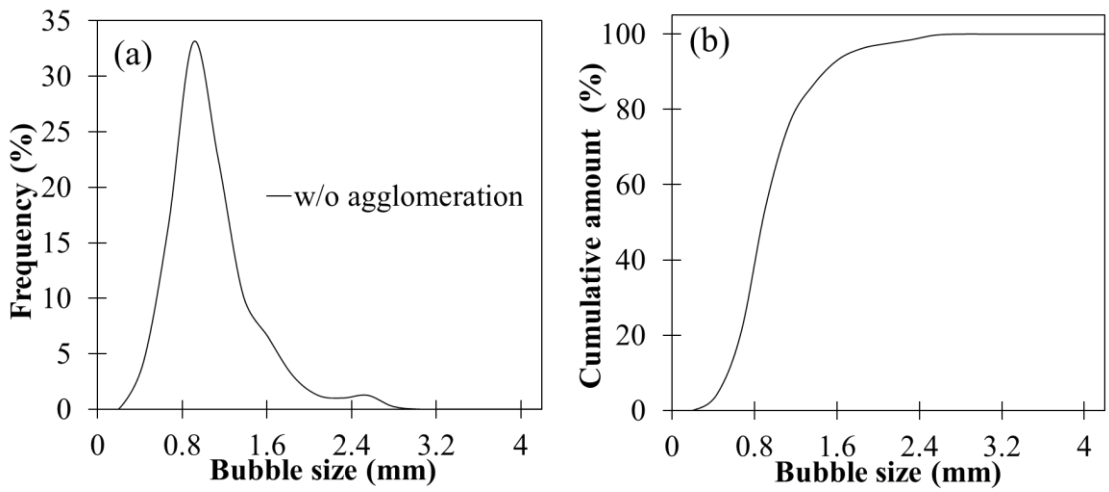

Fig. 3.4. Bubble size (D_b) distribution measured in the filtered flotation solution without oil agglomeration:(a) Frequency (%) as a function of bubble size, and (b) Cumulative (%) as a function of bubble size.

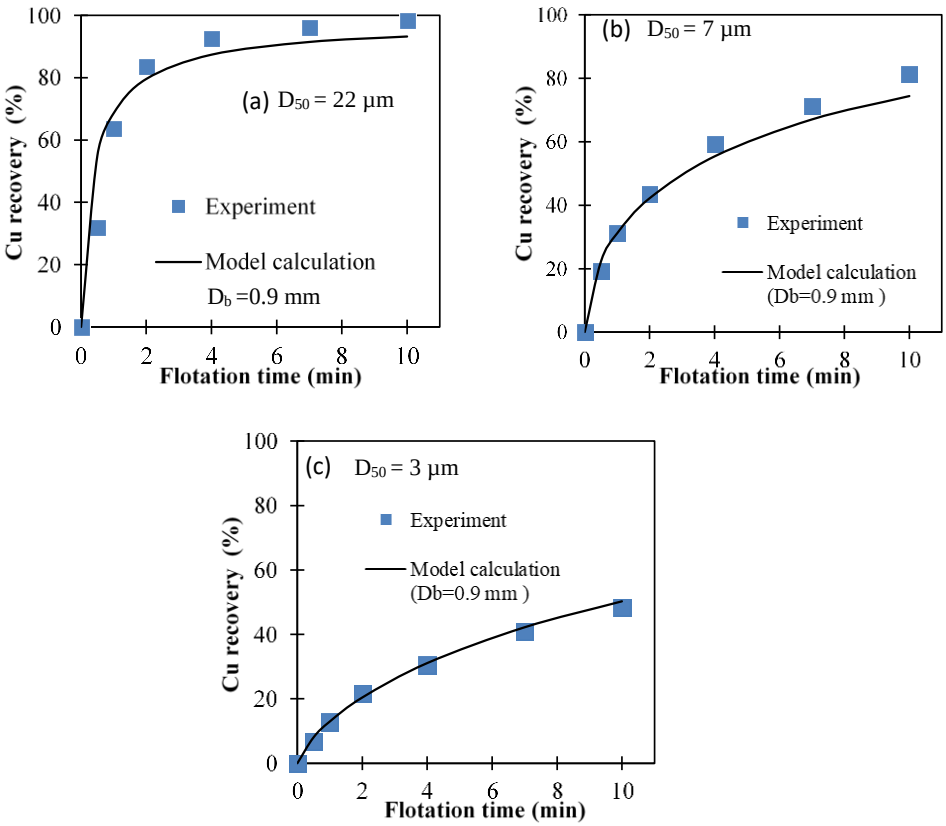

Fig. 3.5. Comparison between experimental flotation results of Samples 1 (D_{50} = 22 µm), 2 (D_{50} = 7 µm) and 3 (D_{50} = 3 µm) and the first-order kinetic model using a bubble size (Db) of 0.9 mm without agglomeration.

3.4.2 Flotation of agglomerated chalcopyrite

Chalcopyrite sample 3 (D_{50} = 3 µm) was used for the agglomeration-flotation tests. Fig. 3.6a and 3.6b show photomicrographs of samples before and after agglomeration, respectively and these results confirmed that the size of particles increased after agglomeration. The accurate size distribution of agglomerate could not be determined from this image because of the limitation of resolution of microscopic observation, which may cause the underrating of the amounts of fine particles. So, we used the laser diffraction sizer, which can measure particle size in the range between 0.02 µm to 2800 µm, to determine the agglomerate size distribution. The particle size distributions (volume-based) without and with agglomeration in terms of frequency and cumulative amount are shown in Figs. 3. 7a and 3.7b, respectively. After agglomeration, the mode particle size increased from 6 to 10 µm and D_{80} increased from 10 µm to 17 µm.

(a) w/o agglomeration (b) w/ agglomeration

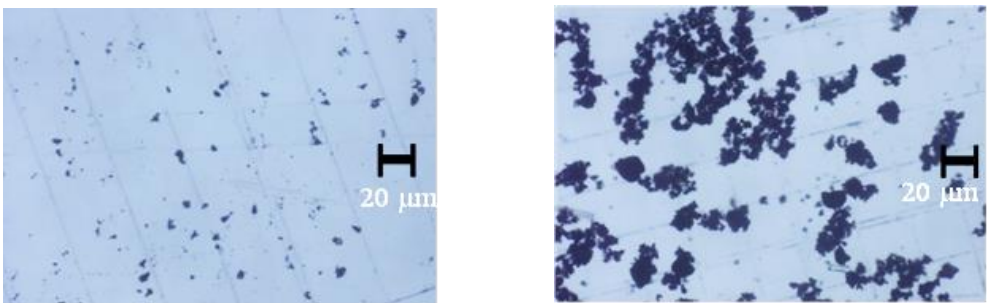

Fig. 3.6. Photomicrographs of finely ground chalcopyrite w/o agglomeration (a) and w/ agglomeration (b).

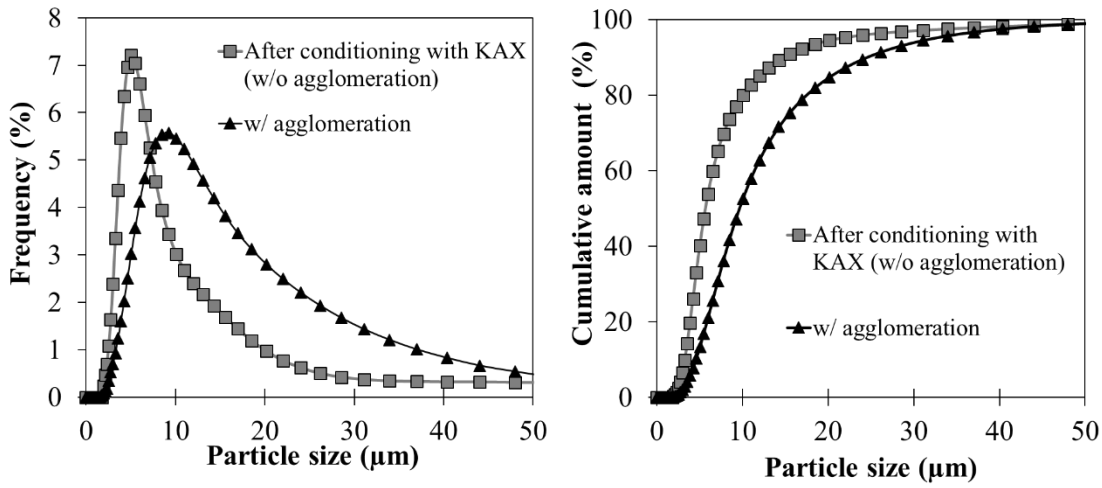

Fig. 3.7. Particle size distribution of sample 3 (D50 = 3 µm) after conditioning with KAX (w/o agglomeration) and w/ agglomeration: (a) frequency as a function of particle size, and (b) cumulative amount as a function of particle size.

Fig. 3.8 shows the Cu recovery as a function of flotation time with and without agglomeration. Copper recovery increased with agglomeration, which indicates that oil agglomeration is an effective technique to improve Cu recovery of finely ground samples.

To evaluate the applicability of the first-order kinetic model to agglomeration-flotation, this model was fitted with the experimental results. In the first trial of the calculation, we assumed that the bubble size is 0.9 mm, which was the same as that previously used in the kinetic model shown in Fig. 3.5, and particle size distribution measured after agglomeration shown in Fig. 3.6 was used. Although the "apparent" density of agglomerates is lower than a single chalcopyrite grain of the same size because agglomerates contain pores, this was ignored for simplicity and the density of agglomerates was assumed to be equal to that of chalcopyrite (4200 kg.m^{-3}).

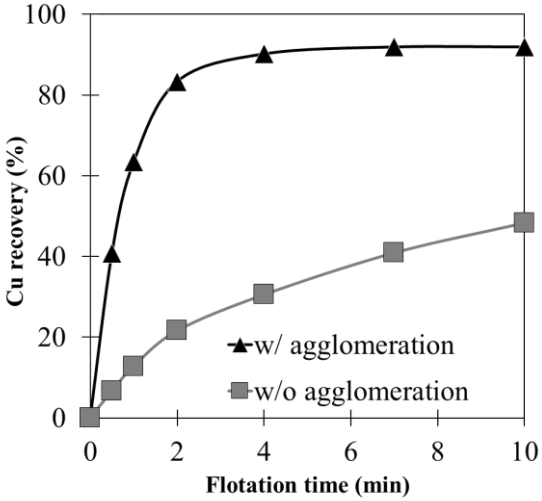

Fig. 3.8. Copper (Cu) recovery as a function of flotation time of Sample 3 (D_{50}= 3 µm) w/o and w/ agglomeration.

Fig. 3.9 shows the calculated results (Cu recovery-time curve) for agglomerated chalcopyrite together with the experimental results. The recovery after 10 min calculated from model was 83% but the experimental results was higher at 92%. This discrepancy indicates that the conventional first-order kinetic model for flotation could was not applicable for agglomerated chalcopyrite.

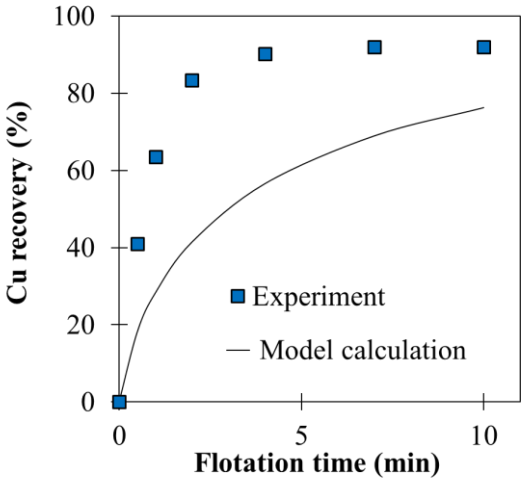

Fig. 3.9. Comparison between the experimental results of agglomerated chalcopyrite and the first-order kinetic model using a bubble size (D_b) of 0.9 mm.

3.4.3 Factors affecting oil agglomeration-flotation

As shown in the conventional first-order kinetic model of flotation (Eq. (3.19)), the kinetic constant

(k_i) of flotation system depends on particle size (D_{pi}), bubble size (D_b), bubble rising velocity (v_b), settling velocity of agglomerate (v_i) and probability of collision (P_{ci}). In the model calculation shown in Fig. 3.9, the values used for D_b, v_b and v_i were only assumed to be the same as used for un-agglomerated chalcopyrite, so to improve the model, these values were experimentally determined. In addition, agglomeration in the flotation cell was also investigated.

*3.4.3.1 Bubble size (**D_b**)*

Bubble size is strongly influenced by the surface tension of water-air interface. During agglomeration, the addition of chemical compounds like kerosene may cause the reduction of surface tension, resulting in smaller bubbles. To evaluate the effects of agglomeration on the surface tension, this parameter was measured in the supernatant after agglomeration of chalcopyrite using a Processor Tensiometer (K100MK2, KRUSS, Germany) at 25°C. The agglomeration condition was 200 g/t of KAX, 0.3 mL of kerosene and 30 min of agglomeration time. The filtrate was collected using filter paper (5C) and 25 μL/L of MIBC was added before the measurement. As summarized in Table 3.1, the surface tension of the filtrate of chalcopyrite suspension after agglomeration was slightly lower than those of distilled water with and without MIBC. Lower surface tension for the filtrate after agglomeration may be due to the formation of surface reducing agent from kerosene and KAX during agglomeration with high speed agitation. The lower surface tension may cause the decrease decay of bubble size in flotation cell.

Bubble size distributions were measured for the filtrate after agglomeration. Fig. 3.10 shows the distribution of bubble size (i.e., diameter) generated in the flotation cell with or without agglomeration after adding 25 μL/L of MIBC as the frother. Although the distribution of bubble size with agglomeration was slightly different compared with the one without agglomeration, the peak bubble size was almost the same (i.e., 0.9 mm) for both cases.

Table. 3.1. Surface tension of various solutions

Solutions	**Surface tension (mN/m)**
D. I water	72.3
D.I water with MIBC (25μl/l)	71.3
Filtrate of ground chalcopyrite suspension after agglomeration	68.5

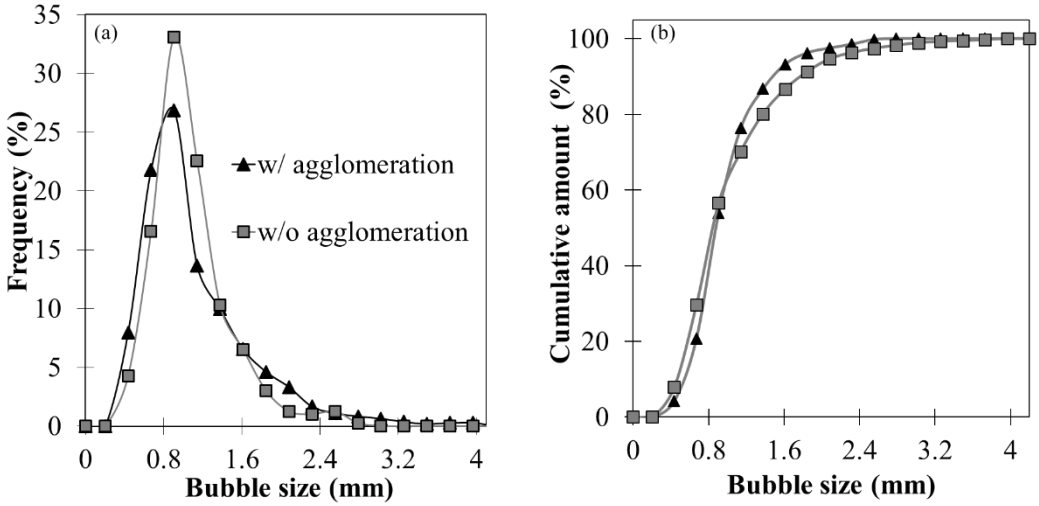

Fig. 3.10. Bubble size (D_b) distribution measured in filtrate solution w/ and w/o agglomeration: (a) Frequency (%), (b) Cumulative (%).

Fig. 3.11 shows the experimental results of flotation for agglomerated chalcopyrite sample with model calculation using different bubble sizes (D_b). To fit the kinetic model with the experimental results, the bubble diameter should be around 0.4 mm. This value is quite different from the actual value shown in Fig. 3.9 (0.9 mm after agglomeration), indicating that the bubble size was not the main reason for the discrepancy between experimental and kinetic modeling results for agglomerated particles.

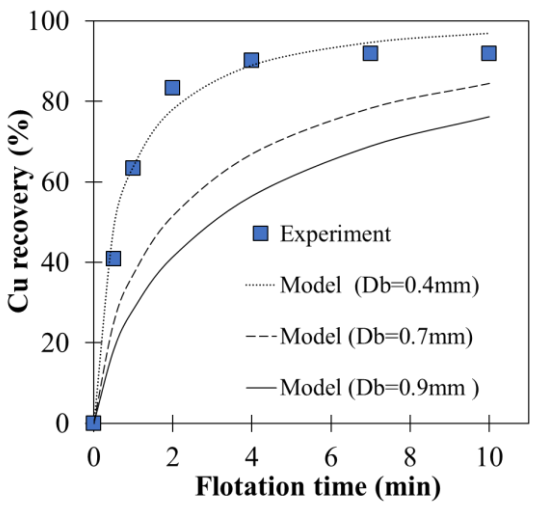

Fig. 3.11. Comparison between agglomeration-flotation experimental results and the kinetic model using different bubble sizes (D_b) of 0.4, 0.7 and 0.9 mm.

3.4.3.2 Bubble rising velocities (v_b)

Fig. 3.12 shows the relation between diameter and rising velocities of air bubbles generated in the flotation cell with or without agglomeration. The bubble rising velocities were measured in the filtrate of agglomeration suspension after adding 25μL/L of MIBC. The results showed that the rising velocities of air bubbles in the filtrate of agglomeration suspension were almost the same as that without agglomeration. The rising velocities of bubbles in both cases were consistent with theoretical values calculated by Eq. (3.12). These results imply that the effects of kerosene used in oil agglomeration on the bubble rising velocities were insignificant. In other words, the changes in bubble rising velocities was not one of the factors that contributed to faster flotation rate of agglomerated particles.

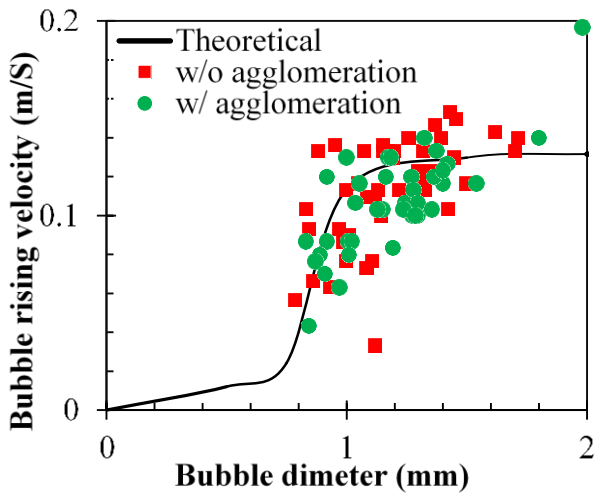

Fig. 3.12. Experimental and model calculated bubble rising velocities in the flotation suspension w/o agglomeration and w/ agglomeration.

3.4.3.3 Settling velocities of agglomerates (v_i)

As mentioned previously, the agglomerate's settling velocity was calculated by assuming that its density was equal to that of chalcopyrite. In reality, however, agglomerates of chalcopyrite are porous, so their apparent density is smaller than that of chalcopyrite. Because of the presence of pores, water to pass through agglomerates, which makes the settling behavior of porous and permeable agglomerates different from that of solid, and impermeable particles (Johnson et al., 1996). These differences may explain the discrepancies observed between the calculated settling velocity and actual velocity. Fig. 3.13 shows the measured value of settling velocity of agglomerated chalcopyrite as a function of diameter of agglomerate. For comparison, calculated values of the settling velocity were also illustrated in this Fig. 3.13. The results showed that agglomerated chalcopyrite settling velocity (SG: 4200 kg·m^{-3}) was lower than the calculated value. As can be seen in Eq. (3.9), the kinetic constant

of flotation is influenced by settling velocities (v_i). When the settling velocity, v_i, becomes larger, the bubble swept volume, $\frac{\pi}{4}(D_b + D_i)^2(v_b + v_i)$, becomes bigger, which results in faster flotation rates as expressed by Eq. (3.9). As shown in Fig. 3.13, the measured settling velocity was lower than that of kinetic model calculation, which caused slower flotation rates. In the actual model calculation, however, the slower settling velocity does not have to be considered because the measured settling velocities (v_i) in Fig. 3. 13 (1–5 μm/s) are significantly lower than the bubble rising velocity (v_b) in Fig. 3.12 (0.02–0.2 m/s). In this case, the bubble swept volume, $\frac{\pi}{4}\left(D_b + D_{pi}\right)^2(v_b + v_i)$, can be approximated as $\frac{\pi}{4}\left(D_b + D_{pi}\right)^2 v_b$, which is independent of v_i. Considering the above, it is reasonable to conclude that the differences between measured and calculated settling velocity does not explain the discrepancies of Cu recovery between experimental and kinetic modeling results.

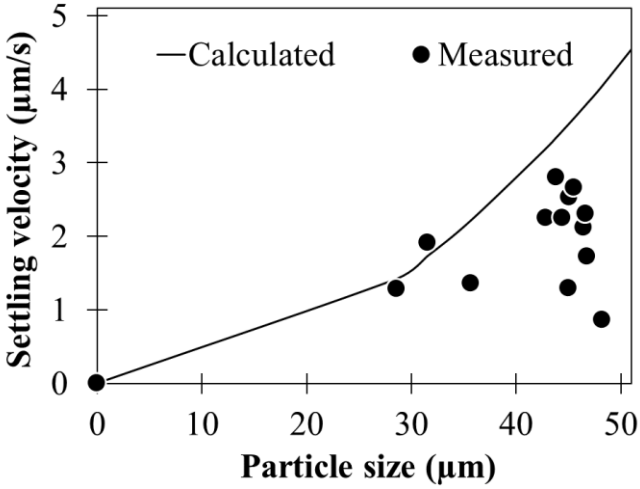

Fig. 3.13. Measured and calculated settling velocity of agglomerated chalcopyrite.

3.4.4 Agglomeration during flotation

It was assumed in the model calculation that agglomeration does not occur in the flotation cell; that is, the size of an agglomerate remains constant during flotation and is equal to that measured after agglomeration (i.e. before flotation). However, agglomeration during flotation could occur because of mechanical agitation in the flotation cell, which induces either breakage of agglomerates or agglomeration of particles. If this is the case, particle size distribution would change during flotation that may explain the discrepancies between experimental and kinetic modeling results. To evaluate the possibility of particle size change in the flotation cell, agglomeration was carried out in the agglomeration vessel and then the suspension was transferred to flotation cell. And then, agglomeration in the flotation cell was carried out and the particle size distribution was measured

without air bubble introduction. For these measurements, the conditions were 200 g/t of KAX, 0.3 mL of emulsified kerosene, 30 min agglomeration vessels and 10 min agglomeration in the flotation cell. Fig. 3. 14 shows the measured particle size distributions, after agglomeration in agglomeration cell, and after agglomeration in agglomeration and flotation cell for 10 min. Agglomeration in the flotation cell for 10 min agitation made the particle size even bigger. These results indicate that oil agglomeration occurred in the flotation cell even if the agitation strength was weaker than that of the high-speed mixer used for agglomeration.

To confirm the effects of the agglomeration in flotation cell, flotation experiments were carried out after agglomeration in the flotation cell. As shown in Fig. 3.15, higher Cu recovery and faster flotation rate were observed after agglomerating in the flotation cell. These results indicate that agglomeration occurred in flotation cell, which caused higher rate and recovery of flotation and explains the discrepancies between experimental and kinetic modeling results noted earlier. This means that agglomeration-flotation could be modeled using a first-order kinetic model by including agglomeration during flotation in the calculations which be discussed in the next section.

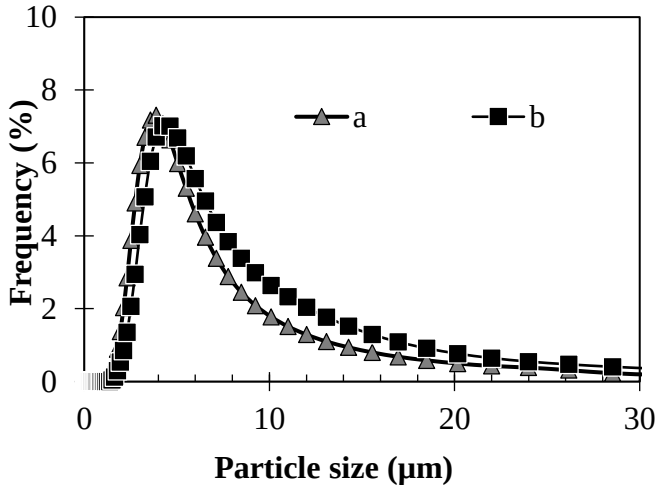

Fig. 3.14. Changes in the particle size distribution of chalcopyrite: (a) after 30 min agglomeration at 15000 rpm, and (b) after 10 min agitation in flotation cell (1000 rpm) of agglomerate pretreated in agglomeration cell (15000 rpm) for 30 min.

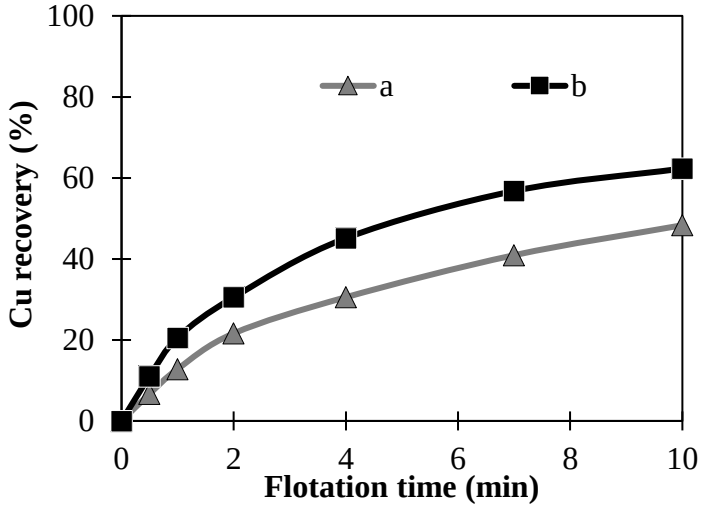

Fig. 3.15. Copper (Cu) recovery as a function of flotation time using sample 3 (D_{50}= 3 μm) chalcopyrite: (a) after 30 min agglomeration at 15000 rpm, and (b) after 10 min agitation in flotation cell (1000 rpm) of agglomerate pretreated in agglomeration cell (15000 rpm) for 30 min.

3.4.5 Proposed model for flotation of agglomerate

As shown in Fig. 3.14, it was confirmed that particle size distribution shifted to coarser size fractions during agitation in flotation cell after agglomeration because the decomposition probability of agglomerates decreases as agitation strength slows down, thus promoting agglomeration in flotation cell where lower agitation strength (1000 rpm) is applied compared to that in agglomeration cell (15000 rpm). This means that a new flotation kinetic model for agglomeration-flotation should include the change in size distribution during flotation in the flotation cell. In the previous model, however, size distributions (η_i) of flotation feed (i.e., agglomerate) were assumed to be unchanged during flotation, which is most likely the primary reason of miss-fitting of the model. To accommodate the change in particle size distribution during flotation after agglomeration into the kinetic model, the actual particle size distribution during flotation of agglomerate was measured. During flotation, froths were recovered at 0.5, 1, 2, 4, 7, and 10 min, and after recovering each froth, air injection was paused, followed by sampling the remaining particles in the pulp for particle size measurements. The size distribution of particle remaining in pulp after each froth recovery was used to calculate the Cu recovery rate of next stage; that is, particle size distributions of pulp remained after recovering the froths at 0.5, 1, 2, 4, and 7 min were used for calculating Cu recovery for 1, 2, 4, 7, and 10 min, respectively. Figure 3.16 shows the newly calculated results comparing with experimental results and conventional kinetic model for flotation. The results indicate that the modified model is better fit with experimental results than that of conventional kinetic model. This means that when the change in apparent size of agglomerate during flotation is considered, model is better fitted with experimental results. Therefore, a new approach that estimates Cu recovery rate of agglomeration-flotation by

measuring the changes in agglomeration size distribution with online monitoring system can be proposed as illustrated in Fig. 3.17.

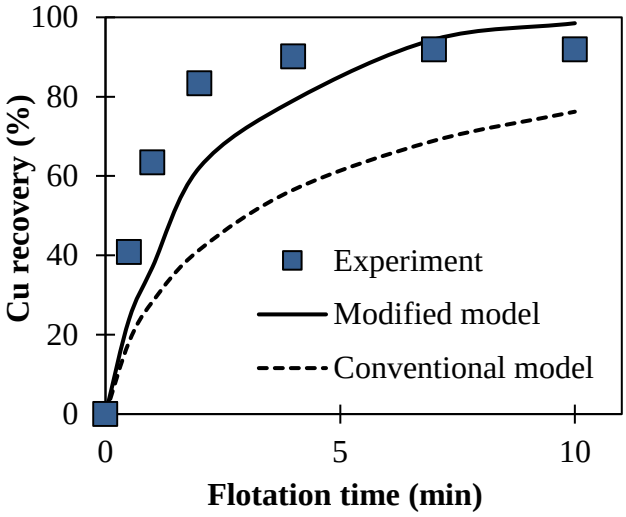

Fig. 3.16 Cu recovery of experimental results of agglomerated chalcopyrite, the conventional first-order kinetic model, and modified firs order kinetic model using a bubble size (D_b) of 0.9 mm.

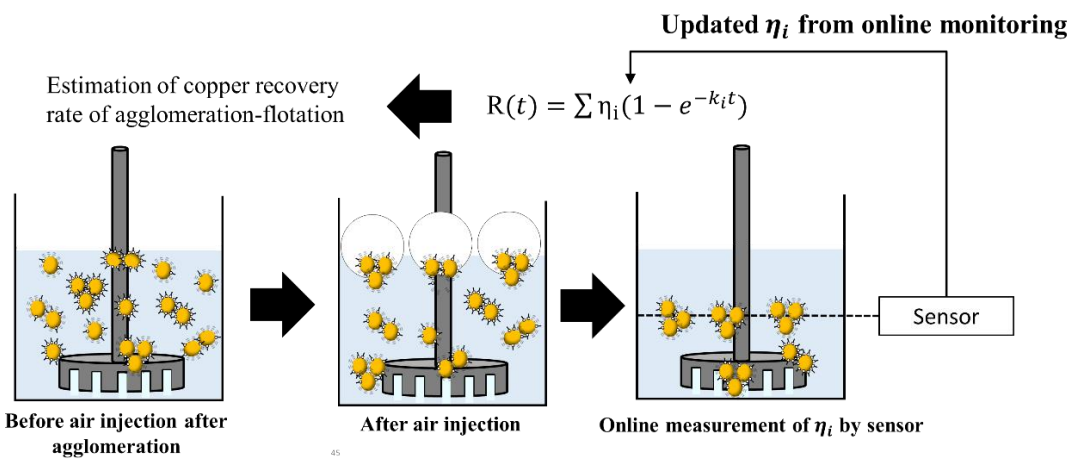

Fig. 3.17 Concept of estimation of Cu recovery rate of agglomeration-flotation using modified kinetic model with online monitoring system.

3.5 Summary

This chapter investigated the agglomeration-flotation behavior of finely ground chalcopyrite experimentally using KAX as surface modifier and kerosene as "bridging" liquid and theoretically using first-order kinetic modeling. The results of this study are summarized as follows:

- Oil-agglomeration before flotation increased the chalcopyrite particle size (D_{50}) from around 6 to 10 μm that dramatically improved the flotation rate.
- Flotation rate that was calculated by first-order kinetic model fitted well with the experimental

results of un-agglomerated chalcopyrite.

- The conventional first-order kinetic model was insufficient to explain the flotation of agglomerated chalcopyrite and model calculated values did not fit the experimental results.
- Bubble size and surface tension, settling rate of agglomerates, bubble rising velocities could not explain the significant deviations between experimental and calculated results.
- Agglomeration occurred in the flotation cell even without prior oil agglomeration in a high-speed mixer and was likely the main reason for the discrepancies between experimental and kinetic modeling results of flotation recovery.
- A new approach to estimate the recovery rate of flotation of agglomerate will be proposed.

This chapter was modified from Hornn et al., (2020) "Kinetic analysis for agglomeration-flotation of finely ground chalcopyrite: Comparison of first order kinetic model and experimental results. Materials Transactions (Accepted July 2020).

Notation

D_i: Diameter of particle type i

D_b: Diameter of bubble

P_A : Probabilities of particle/ bubble attachment

P_D : Probabilities of particle/bubble detachment

P_C : Probabilities of particle/bubble collision

G_v : Specific aeration rate

k_i: Kinetic constant of particle type i

n_b: Number of bubbles in flotation cell

η_i: Particle distribution frequency (%) of particle type i

Re_b: Reynold number of bubbles

R: Copper recovery (%)

t: Flotation time (s)

v_b: Bubble rising velocity

v_i: Particle settling velocity

References

Alonso, M. I., Valdés, A. F., Martínez-Tarazona, R. M., and Garcia, A. B. (1999). Coal recovery from coal fines cleaning wastes by agglomeration with vegetable oils: Effects of oil type and concentration. *Fuel*, *78*(7), 753–759. https://doi.org/10.1016/S0016-2361(98)00218-X

Bensley, C. N., Swanson, A. R., and Nicol, S. K. (1977). The effect of emulsification on the selective agglomeration of fine coal. *International Journal of Mineral Processing*, *4*(2), 173–184.

https://doi.org/10.1016/0301-7516(77)90024-2

Bhaskar Raju, G., and Khangaonkar, P. R. (1982). Electro-flotation of chalcopyrite fines. *International Journal of Mineral Processing*, *9*(2), 133–143. https://doi.org/10.1016/0301-7516(82)90022-9

Dai, Z., Fornasiero, D., and Ralston, J. (2000). Particle–bubble collision models—A review. *Advances in Colloid and Interface Science*, *85*(2), 231–256. https://doi.org/10.1016/S0001-8686(99)00030-5

Finch, J. A. (1995). Column flotation: A selected review— part IV: Novel flotation devices. *Minerals Engineering*, *8*(6), 587–602. https://doi.org/10.1016/0892-6875(95)00023-J

Grau, R. A., and Heiskanen, K. (2002). Visual technique for measuring bubble size in flotation machines. *Minerals Engineering*, *15*(7), 507–513. https://doi.org/10.1016/S0892-6875(02)00074-2

Grau, R. A., and Heiskanen, K. (2003). Gas dispersion measurements in a flotation cell. *Minerals Engineering*, *16*(11), 1081–1089. https://doi.org/10.1016/j.mineng.2003.06.007

House, C. I., and Veal, C. J. (1989). Selective recovery of chalcopyrite by spherical agglomeration. *Minerals Engineering*, *2*(2), 171–184. https://doi.org/10.1016/0892-6875(89)90038-1

Jiangang, F., Kaida, C., Hui, W., Chao, G., and Wei, L. (2012). Recovering molybdenite from ultrafine waste tailings by oil agglomerate flotation. *Minerals Engineering*, *39*, 133–139. https://doi.org/10.1016/j.mineng.2012.07.006

Johnson, C. P., Li, X., and Logan, B. E. (1996). Settling Velocities of Fractal Aggregates. *Environmental Science and Technology*, *30*(6), 1911–1918. https://doi.org/10.1021/es950604g

King, R. P. (2001). Flotation (Section 9.2). In *Modeling and Simulation of Mineral Processing Systems* (pp. 312–313). Elsevier.

Li, X., Hiroyoshi, N., Tabelin, C. B., Naruwa, K., Harada, C., and Ito, M. (2019). Suppressive effects of ferric-catecholate complexes on pyrite oxidation. *Chemosphere*, *214*, 70–78. https://doi.org/10.1016/j.chemosphere.2018.09.086

Miettinen, T., Ralston, J., and Fornasiero, D. (2010). The limits of fine particle flotation. *Minerals Engineering*, *23*(5), 420–437. https://doi.org/10.1016/j.mineng.2009.12.006

Park, I., Tabelin, C. B., Magaribuchi, K., Seno, K., Ito, M., and Hiroyoshi, N. (2018). Suppression of the release of arsenic from arsenopyrite by carrier-microencapsulation using Ti-catechol complex. *Journal of Hazardous Materials*, *344*, 322–332. https://doi.org/10.1016/j.jhazmat.2017.10.025

Polat, M., and Chander, S. (2000). First-order flotation kinetics models and methods for estimation of the true distribution of flotation rate constants. *International Journal of Mineral Processing*, *58*(1), 145–166. https://doi.org/10.1016/S0301-7516(99)00069-1

Rodrigues, R. T., and Rubio, J. (2007). DAF–dissolved air flotation: Potential applications in the mining and mineral processing industry. *International Journal of Mineral Processing*, *82*(1), 1–13. https://doi.org/10.1016/j.minpro.2006.07.019

Rubio, J., and Hoberg, H. (1993). The process of separation of fine mineral particles by flotation with hydrophobic polymeric carrier. *International Journal of Mineral Processing*, *37*(1), 109–122. https://doi.org/10.1016/0301-7516(93)90008-X

Sahinoglu, E., and Uslu, T. (2013). Use of ultrasonic emulsification in oil agglomeration for coal cleaning. *Fuel*, *113*, 719–725. https://doi.org/10.1016/j.fuel.2013.06.046

Slaghuis, J. H., and Ferreira, L. C. (1987). Selective spherical agglomeration of coal. *Fuel*, *66*(10), 1427–1430. https://doi.org/10.1016/0016-2361(87)90191-8

Song, S., Lopez-Valdivieso, A., Reyes-Bahena, J. L., and Lara-Valenzuela, C. (2001). Floc flotation of galena and sphalerite fines. *Minerals Engineering*, *14*(1), 87–98. https://doi.org/10.1016/S0892-6875(00)00162-X

Sresty, G. C., and Somasundaran, P. (1980). Selective flocculation of synthetic mineral mixtures using modified polymers. *International Journal of Mineral Processing*, *6*(4), 303–320. https://doi.org/10.1016/0301-7516(80)90027-7

Tabelin, C. B., Veerawattananun, S., Ito, M., Hiroyoshi, N., and Igarashi, T. (2017). Pyrite oxidation in the presence of hematite and alumina: I. Batch leaching experiments and kinetic modeling calculations. *Science of The Total Environment*, *580*, 687–698. https://doi.org/10.1016/j.scitotenv.2016.12.015

Trahar, W. J. (1981). A rational interpretation of the role of particle size in flotation. *International Journal of Mineral Processing*, *8*(4), 289–327. https://doi.org/10.1016/0301-7516(81)90019-3

Trahar, W. J., and Warren, L. J. (1976). The flotability of very fine particles—A review. *International Journal of Mineral Processing*, *3*(2), 103–131. https://doi.org/10.1016/0301-7516(76)90029-6

van Netten, K., Moreno-Atanasio, R., and Galvin, K. P. (2016). Selective agglomeration of fine coal using a water-in-oil emulsion. *Chemical Engineering Research and Design*, *110*, 54–61. https://doi.org/10.1016/j.cherd.2016.02.029

Vinnett, L., Alvarez-Silva, M., Jaques, A., Hinojosa, F., and Yianatos, J. (2015). Batch flotation kinetics: Fractional calculus approach. *Minerals Engineering*, *77*, 167–171. https://doi.org/10.1016/j.mineng.2015.03.020

Warren, L. J. (1975). Shear-flocculation of ultrafine scheelite in sodium oleate solutions. *Journal of Colloid and Interface Science*, *50*(2), 307–318. https://doi.org/10.1016/0021-9797(75)90234-9

Yalcin, E., and Kelebek, S. (2011). Flotation kinetics of a pyritic gold ore. *International Journal of*

Mineral Processing, *98*(1), 48–54. https://doi.org/10.1016/j.minpro.2010.10.005

Yoon, R. H. (2000). The role of hydrodynamic and surface forces in bubble–particle interaction. *International Journal of Mineral Processing*, *58*(1–4), 129–143. https://doi.org/10.1016/S0301-7516(99)00071-X

Yoon, R.-H. (1993). Microbubble flotation. *Minerals Engineering*, *6*(6), 619–630. https://doi.org/10.1016/0892-6875(93)90116-5

Yoon, R.H., and Lutttrell, G. H. (1989). The Effect of Bubble Size on Fine Particle Flotation. *Mineral Processing and Extractive Metallurgy Review*, *5*(1–4), 101–122. https://doi.org/10.1080/08827508908952646

CHAPTER 4: EFFECTS OF AGITATION STRENGTH DURING AGGLOMERATION

4.1 Introduction

In coal cleaning, high speed mixer and kitchen blender are used to selectively agglomerate coal and to remove gangue minerals trapped in agglomerates. Thus, high speed mixer was used in chapter three. Although high agitation during agglomeration improved Cu recovery, it requires high energy consumptions, which make the process costly. In this chapter, effects of agitation strength during agglomeration was investigated. In the experiments, two-step process, consisting of (1) KAX (potassium amyl xanthate) conditioning in the conditioning cell and (2) agglomeration with emulsified oil in the agglomeration vessel prior to flotation was applied. Effects of agitation strength during agglomeration, dosage of KAX as surface modifier and dosage of oil as bridging liquid are investigated. In addition, separation efficiency of chalcopyrite and quartz by agglomeration-flotation using emulsified oil is evaluated.

4.2 Materials and methods

4.2.1 Materials

Two samples were used in this study: chalcopyrite and quartz. Chalcopyrite sample was obtained from Copper Queen Mine, Arizona, USA while quartz sample (99% of purity) was obtained from Wako Pure Chemical Industries Co., Ltd., Japan. Chalcopyrite sample was characterized using X-ray fluorescence (XRF) (EDXL300, Rigaku Corporation, Japan) and X-ray powder diffraction (XRD, Multiplex, Rigaku Corporation, Japan). Elemental composition of the sample is shown in Table. 4.1. XRD analysis indicated that chalcopyrite is the major mineral while actinolite ($Ca_2Mg_3Fe_2Si_8O_{22}(OH)_2$), quartz and sphalerite are minor minerals.

Chalcopyrite specimen was crushed using a jaw crusher (1023-A, Yoshida Manufacturing co., Ltd, Japan) and ground by a vibratory disc mill (RS100, Retsch Inc., Germany), then screened to obtain a size fraction of less than 75 µm. The ground sample (less than 75 µm) was ground again by the vibratory disc mill to obtain fine particles having median particle diameter (D_{50}) of 3.5 µm. The quartz sample (primary particle dimeter of less than 500 µm) was ground separately in the same manner as the chalcopyrite sample. The median particle diameter (D_{50}) of the quartz sample was 6 µm. The particle distribution of chalcopyrite and quartz sample used in this study were measured in water after ultrasonication (Fig. 4.1) using a laser diffraction machine (Microtrac® MT3300SX, Nikkiso Co., Ltd., Japan).

Potassium amyl xanthate (KAX) (Tokyo Chemical Industry Co., Ltd., Japan), Kerosene (Wako Pure Chemical Industries, Ltd., Japan) and Methyl Isobutyl Carbinol (MIBC), (Tokyo Chemical

Industry Co., Ltd., Japan) were used in this study.

Table. 4 1. Chemical composition of chalcopyrite sample.

Elements	Cu	Fe	S	Zn	Si	Ca
wt%	26	27	26	0.8	6	2

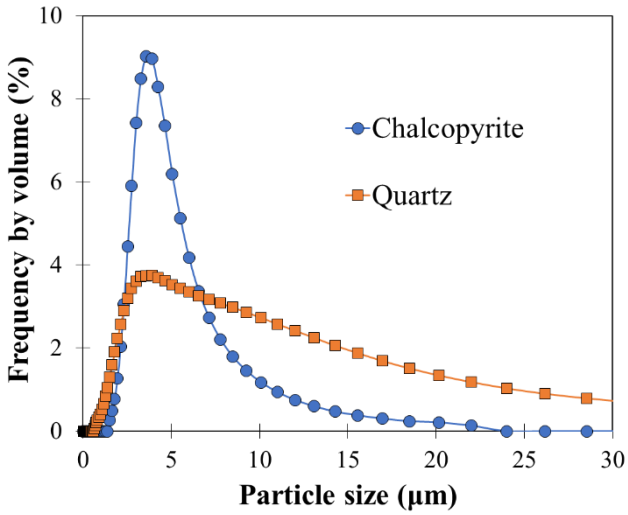

Fig. 4.1. Particle size distribution of crushed chalcopyrite and quartz.

4.2.2 KAX conditioning in the conditioning cell and agglomeration in the agglomeration vessel

KAX conditioning and agglomeration were conducted on finely ground chalcopyrite sample (D_{50}= 3.5 µm) or mixture of finely ground chalcopyrite and quartz (D_{50}= 6 µm) at the ratio of 1:1 (w/w). Before agglomeration, 20 g of samples were suspended in 400 mL of distilled water, then the suspension was conditioned with the surface modifier, KAX (50, 200 or 1000 g/t) for 5 minutes at 1000 rpm in the flotation cell (FT-1000, Heiko, Japan). After conditioning, the suspension was transferred to an agglomeration vessel, emulsified oil (0, 15 or 25 L kerosene/t sample) was then added and agitation was carried out for 30 minutes with a predetermined stirring speed (1000, 4000, or 15000 rpm). Two types of agglomeration machines were used: (machine A) a rotary stirrer (B.NR 301, Heidolph, Germany; rotation speed of 0–5000 rpm) with a two-bladed impeller and a cylinder vessel, and (machine B) a high speed mixer with a s-shape impeller (SPB-600J, Cuisinart, USA; fix rotation speed of 15000 rpm). Agglomeration was conducted for 30 minutes using agglomeration machine A at 1000 and 4000 rpm, and agglomeration machine B at 15000 rpm. The suspension containing agglomerates was transferred to a flotation cell and the flotation experiments were carried out.

4.2.3 Flotation tests

Suspension after agglomeration was transferred to a 500 mL flotation cell. Flotation was carried out using a mechanical flotation machine (FT-1000, Heiko, Japan). MIBC (25 μL/L) was added as a frother and the suspension was stirred for 3 minutes with an impeller speed of 1000 rpm. Air was then injected to the suspension at a flow rate of 1 L/min and flotation was carried out (total flotation time of 10 min). Froths were collected at predetermined time intervals, and both froth products and tailings were weighed after drying at 105°C for 24 h and their elemental compositions were determined using an XRF.

4.3 Results and discussion

4.3.1 Effects of agitation strength

Agitation strength is an important factor for agglomeration of hydrophobic particles using oil as bridging liquid. Agglomeration kinetics and agglomerate size are mainly determined by (1) particle-particle collision, (2) particle-particle attraction, and (3) decomposition of agglomerate. Among them, probabilities of particle-particle collision (1) and agglomerate decomposition (3) are directly affected by agitation strength; that is, when agitation become strong, both collision and decomposition probabilities are increased.

Particle-particle attraction (2) is also indirectly affected by agitation strength. The attraction force is determined by hydrophobic interaction between hydrophobic surfaces and capillary force of bridging liquid between particle and particle; that is, the former is improved by the addition of KAX while the latter is affected by the size of oil droplets attached on the surface of particles. In the case of capillary force, it is generated by bridging liquid, which bridges particle and particle after collision of particles occurs. However, when the size of oil droplets is too big, the capillary force becomes weak, and thus suitable conditions (e.g., funicular state and capillary state) (Mort, 2005) are desired to maximize capillary force. Moreover, probability of attachment between particle and particle after collision is proportional to the number of oil droplets attached on the surface of particle. In short, particle-particle attraction (2) is affected by the size and number of oil droplets attached on the surface of particles, both of which are controlled by agitation strength; for instance, high agitation strength produces small size and large number of oil droplets in suspension. Considering these things, the effects of agitation strength on oil droplet size, agglomerate size, and flotation recovery of agglomerated chalcopyrite were investigated.'

Fig. 4.2 shows the size distribution of oil droplets. In this experiment, 20 mL of emulsified oil (20% kerosene, as explained in section 2.2) was added into 380 mL distilled water and agitated for 30 min by the agglomeration machine. The size distribution of oil droplets generated by machine B (15000 rpm) was shifted to smaller fractions compared to that generated by machine A (1000 rpm);

that is, mode sizes (i.e., peak sizes) were about 10 µm with machine B and 24 µm with machine A. This is due to the stronger shear force by machine B: Oil droplet was split by the shear force and the size became smaller.

Fig. 4. 3 shows the size distribution with and without agglomeration. Before agglomeration, 20 g of samples were suspended in 400 mL of distilled water, then the suspension was conditioned with the surface modifier, KAX (200 g/t) for 5 minutes at 1000 rpm in the flotation cell. After KAX conditioning, the suspension was transferred to an agglomeration vessel, emulsified oil (15 L kerosene/t sample) was then added and agitation was carried out for 30 minutes with a predetermined stirring speed (1000 or 15000 rpm). The results showed that apparent particle sizes increased after agglomeration based on the increases in frequency of coarser fractions, indicating that agglomeration occurred. However, there is no significant difference in the size distributions with machine A and machine B.

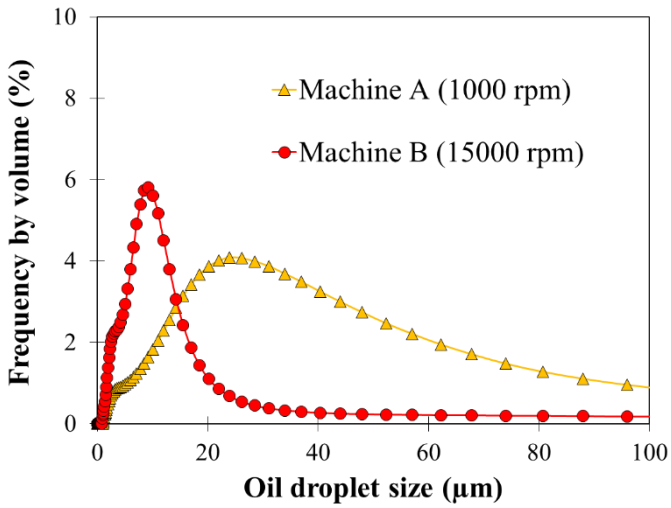

Fig. 4.2. Size distribution of oil droplets in suspension (1 wt% of kerosene and 99 wt% of distilled water) prepared using machine A (1000 rpm) and B (15000 rpm).

Fig. 4.4 shows flotation results with and without agglomeration. In the case of flotation without agglomeration (i.e., control), after conditioning with 200 g/t of KAX and 25 µL/L of frother, emulsified oil (15 L kerosene/t sample) was added and then immediately flotation was conducted. Even when emulsified oil was added after conditioning with KAX and frother (control), the result showed lower recovery rather than that with agglomeration. These results indicate that not only the addition of emulsified oil but also agglomeration treatment is essential for improving the flotation recovery.

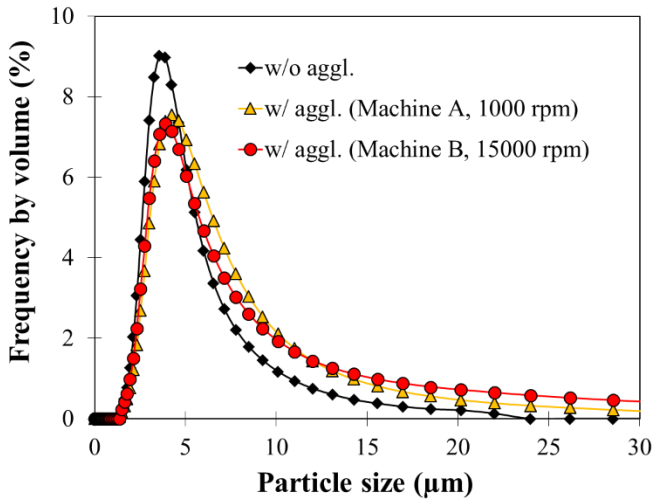

Fig. 4.3. Size distribution of of chalcopyrite without agglomeration and with agglomeration using machine A (1000 rpm) and machine B (15000 rpm).

When agglomeration was applied, higher Cu recovery was obtained. Cu recovery with agglomeration using machine B was higher than that with machine A. Flotation kinetics mainly depends on particle size and hydrophobicity (Feng and Aldrich, 1999; Hornn et al., 2019; King, 2001b; Muganda et al., 2011; Trahar and Warren, 1976) and agglomeration technique can improve flotation kinetics due to increase of apparent size resulted in high Cu recovery with agglomeration treatment (Fig. 4.4). Based on these results, the detailed mechanisms of how agglomeration-flotation with emulsified oil improves the Cu recovery can be proposed as follows.

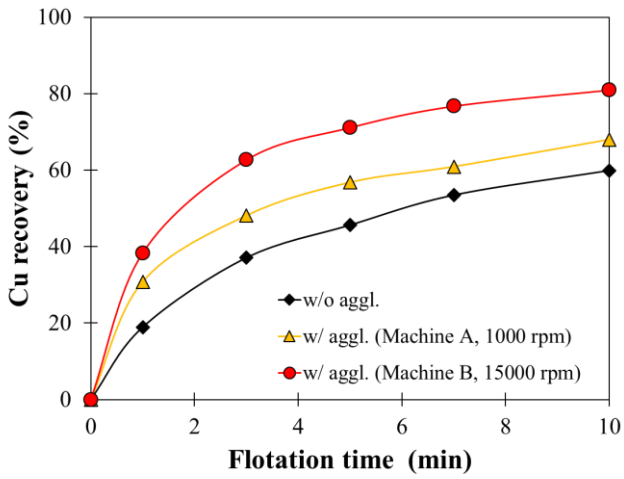

Fig. 4. 4. Cu recovery without agglomeration and with agglomeration using machine A (1000 rpm) and machine B (15000 rpm).

Effects of agitation strength on oil droplets during agglomeration: During agitation, oil droplets were split by the shear force and the size became smaller as shown in Fig. 4.2. When the size of oil droplets become smaller, the number of droplets in the agitator increases, so stronger agitation energy

can produce a large number of oil droplets. Frequency of collision of the oil droplets and particles in agglomeration system is proportional to the number of oil droplets and relative velocity to approach to each other, so it is reasonable to assume that the number of oil droplets attached on particle surface, induced by the collision of oil droplet and particle, become larger when stronger agitation condition is applied. This would affect the agglomeration process and the flotation of the agglomerate.

Effects of agitation strength on agglomeration and flotation: Flotation kinetics mainly depends on particle size and hydrophobicity (Feng and Aldrich, 1999; Hornn et al., 2019; King, 2001b; Muganda et al., 2011; Trahar and Warren, 1976), so agglomeration technique can improve flotation kinetics due to increase of apparent size resulted in high Cu recovery with agglomeration treatment (Fig. 4.4). Agglomerate sizes were similar with agglomeration machine A and B (Fig. 4.3), indicating that the difference in Cu recovery is not due to the difference in agglomerate size. As discussed previously, the number of oil droplets attached to mineral surface may be larger when using the agitation machine B (15000 rpm), and it may cause that probability of attachment between mineral particles after collision becomes larger, so the agglomeration could be enhanced. Under a stronger agitation condition in machine B (15000 rpm), however, decomposition of agglomerate would be also enhanced. This may be a reason why agglomerate size in machine B (15000 rpm) is almost the same as that in machine A (1000 rpm). Even with the similar agglomerate size, the number of oil droplets attached on the mineral surface may be different: a larger number of oil droplets are attached on the mineral surface when machine B was used. This may cause a more hydrophobic surface and enhanced Cu recovery.

Agglomeration with both agglomeration machine A and B is effective to improve the recovery of finely ground chalcopyrite particles.

4.3.2 Effects of kerosene dosage

Effects of kerosene dosage on agglomerate size and flotation of agglomerate were investigated. In the case of kerosene dosage of 0 L kerosene/t sample, conditioning with KAX (200 g/t) was conducted for 5 minutes at 1000 rpm in the flotation cell, then the suspension was transferred to an agglomeration vessel and agitated for 30 minutes without the addition of emulsified oil. Fig. 4. 5 shows the effects of kerosene dosage on median diameter (D_{50}) of agglomerates. As shown in Fig. 4. 5, at agitation speed of 1000 rpm and 4000 rpm, median diameter of agglomerate was less dependent on kerosene dosage, while the median diameter increased with increasing kerosene dosage when agitated at 15000 rpm. As already discussed, when low speed agitation is applied, the number of oil droplets attached to mineral surface is limited, and this may be the reason why agglomerate size is less dependent on kerosene dosage. When high agitation speed was applied, the number of oil droplets increased due to the decrease in the size of oil droplets, causing a high collision frequency between oil droplets and mineral particles. This causes an increase in the number of attached oil droplets on the mineral surface when kerosene dosage increases. As a result, median size of agglomerate increased with increasing kerosene

dosage when high speed agitation was applied.

Fig. 4.6 shows Cu recovery after 10 min flotation of agglomerate under varied agitation strength. As shown in Fig. 4.6, when emulsified oil was not added to the agglomeration process, Cu recovery was not affected by varying agitation strengths. Moreover, at low agitation strength (i.e., 1000 rpm and 4000 rpm), Cu recovery showed similar value even if kerosene dosage increased. Comparing with the result of median diameter, Cu recovery were well corelated to the agglomerate size: at low speed agitation (1000 rpm and 4000 rpm), agglomerate size was relatively small regardless of the kerosene dosage, causing a low Cu recovery. When high speed agitation (15000 rpm) and larger kerosene dosage were applied, agglomerate size became larger, resulting in high Cu recovery. This result agrees with the reported findings about flotation kinetics (Feng and Aldrich, 1999) a faster flotation rate is achieved for larger particles due to a high collision probability between particle and air bubble.

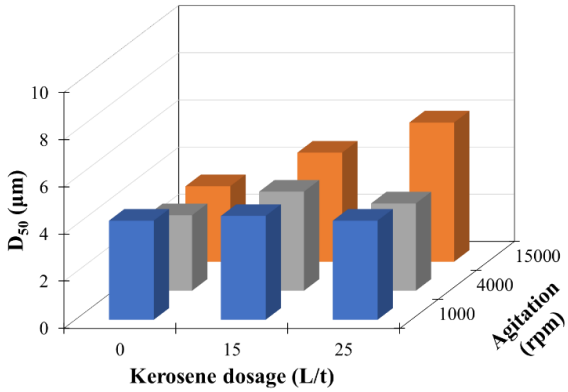

Fig. 4.5. Effects of kerosene dosage and agitation speed on median diameter (D_{50}) of agglomerates (KAX 200 g/t).

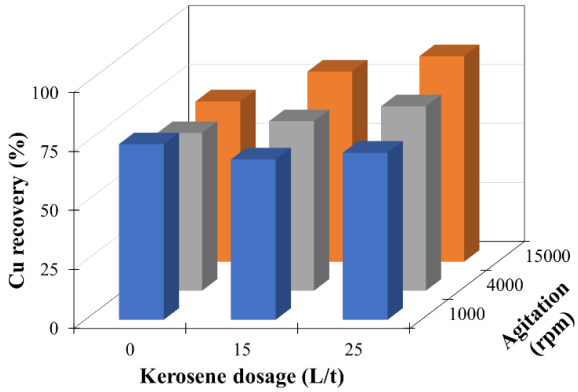

Fig. 4.6. Effects of kerosene dosage and agitation speed on Cu recovery (KAX 200 g/t, flotation time 10 min)

.

4.3.3 Effects of KAX dosage

Effects of KAX dosage on agglomerate size and flotation of agglomerate were investigated under varied agitation conditions. Fig. 4.7 shows the effects of KAX dosage on median diameter (D_{50}) of agglomerates. The dosage of kerosene was fixed to be 15 L kerosene/t sample. As shown in Fig. 4.7, median diameter of agglomerate slightly increased with increasing KAX dosage at agitation speed of 1000 rpm and 4000 rpm, while the effect become significant at 15000 rpm. There are two possible mechanisms of how KAX addition contributes to agglomeration: (1) increasing hydrophobic interaction between particles, and (2) increasing attachment probability of particle and oil droplet. Chalcopyrite surface become hydrophobic when KAX is adsorbed on the mineral surface, and the increase in the adsorption amount of KAX may cause a strong hydrophobic interaction between particles, and thus median size of agglomerates becomes bigger. In addition, when the mineral surface is rendered hydrophobic, the attachment probability after collision of oil droplet and mineral surface is increased, and thus median size of agglomerates becomes bigger. These results indicate that median diameter of agglomerate was affected by not only kerosene as bridging liquid but also KAX amount as surface modifier.

Fig. 4.8 shows Cu recovery after 10 min flotation of agglomerate under varied agitation strength. This result shows that Cu recovery increased with increasing both KAX dosage and agitation speed. High Cu recovery at high speed agitation with a large KAX dosage can be interpreted based on a larger size of the agglomerate; for example, at 15000 rpm with 1000 g/t KAX, both agglomerate size and Cu recovery become highest. At 1000 rpm, however, Cu recovery increased but agglomerate size was slightly increased with increasing KAX dosage. In addition, as described previously, the increase of KAX addition assists the attachment probability of oil droplet and mineral surface, resulting in the number of oil droplets attached on mineral surface increases, which improve hydrophobicity of agglomerate even median diameter shows similar values. Thus, Cu recovery could be significantly increased although the median diameter of agglomerate was slightly increased with increasing KAX dosage (Figs. 4.7 and 4.8).

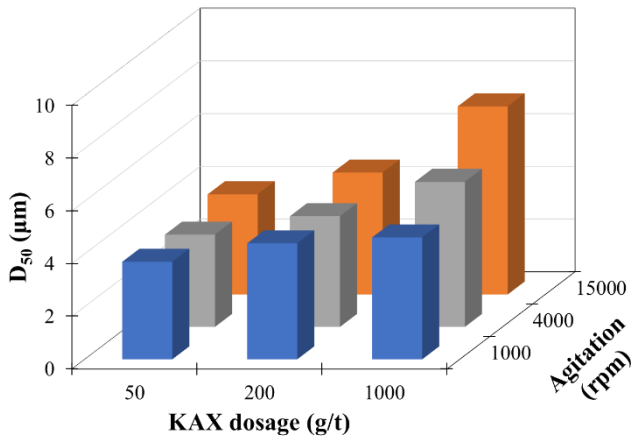

Fig. 4.7. Effects of KAX dosage and agitation speed on median diameter (D_{50}) of agglomerates (Kerosene 15 L kerosene/t sample).

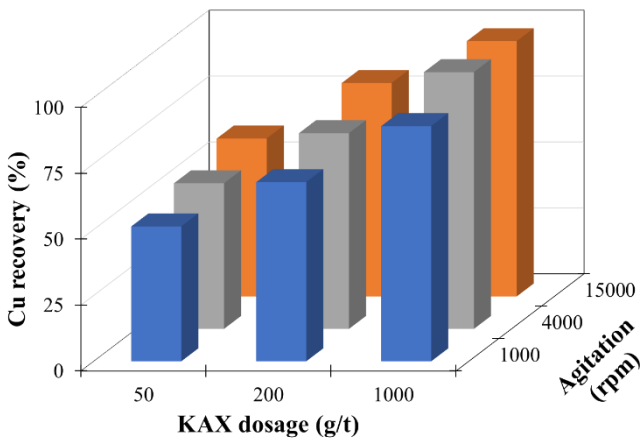

Fig. 4.8. Effects of KAX dosage and agitation speed on Cu recovery (Kerosene dosage 15 L kerosene/t sample, flotation time 10 min).

4.3.4 Separation of finely ground chalcopyrite and quartz by agglomeration-flotation

In actual flotation of copper sulfide ores, the ore contains copper (chalcopyrite) and gangue minerals like quartz. To investigate effects of agitation strength, KAX dosage, kerosene dosage on separation efficiency, agglomeration-flotation experiments were conducted using a mixture of 10 g of chalcopyrite and 10 g of quartz. One of the effects of coexistence of quartz during flotation is entrapment of quartz in agglomerate, resulting in high recovery of quartz in froth. This may cause the decrease of separation efficiency. Flotation kinetics is mainly determined by (1) particle-bubble collision, (2) particle-bubble attachment, and (3) detachment of particle from a bubble. Coexistence of quartz is possible to affect the flotation kinetics, which can be explained by the following possibilities. The size distribution of finely ground chalcopyrite after agglomeration in the absence

and presence of quartz would be different, which means that (1) collision probability of particle-bubble may also be changed. When quartz is entrapped in agglomerate, contact angle of agglomerate may decrease, so (2) attachment and (3) detachment probabilities of particle-bubble will change. According to the flotation results comparing with and without quartz, however, flotation kinetic as well as Cu recovery showed similar values (about 80% Cu recovery) under the condition of 200 g/t KAX, 25 L kerosene/t sample kerosene and 15000 rpm, indicating that the presence of quartz does not affect the Cu recovery.

4.3.4.1 Effects of KAX dosage and agitation strength on separation efficiency

Fig. 4. 9 shows the relationship between Cu recovery in froth, R_{Cu} (%), and Si recovery in tailings, R_{Si} (%), after agglomeration-flotation under the following conditions: kerosene dosage, 15 L kerosene/t sample; agglomeration time, 30 min; agitation strength, 1000 rpm and 15000 rpm; KAX dosage, 200g/t and 1000 g/t. In the case of flotation without agglomeration (i.e., control), flotation was conducted after conditioning with KAX and 25 μL/L of frother.

With increasing agitation strength and KAX dosage Cu recovery increased significantly while Si recovery in tailings was almost constant (around 20%). The separation efficiency, η (%), which can be defined by Eq. (4.1), increased with increasing agitations strength and KAX dosage. These results indicate that quartz may not affect the Cu recovery. Even with presence of quartz, Cu recovery increase with increasing agitation strength and KAX dosage, resulting in the improvement of separation efficiency.

$$\eta\ (\%) = R_{Cu}\ (\%) + R_{Si}\ (\%) - 100 \qquad (4.1)$$

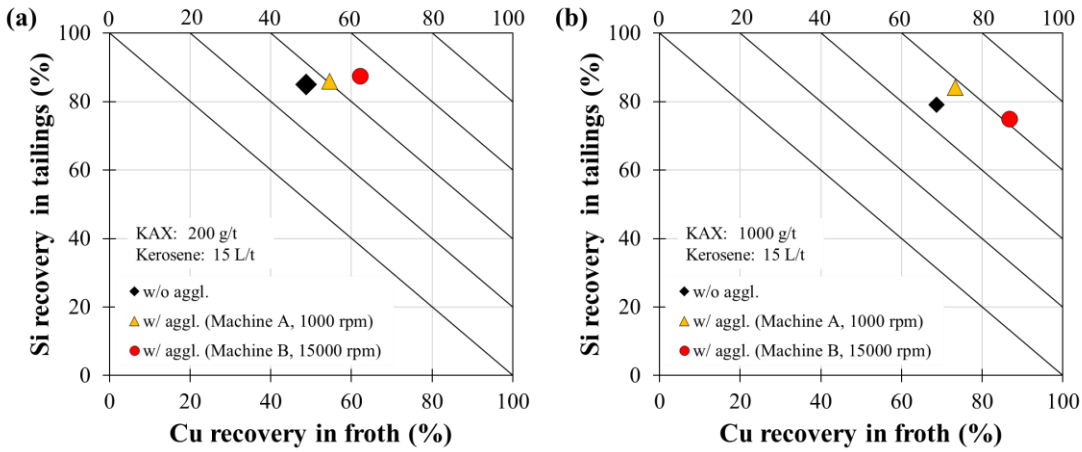

Fig. 4.9. Relationship between Cu recovery in froth, R_{Cu} (%), and Si recovery in tailing, R_{Si} (%), of chalcopyrite and quartz mixture with different KAX dosage: (**a**) 200 g/t and (**b**) 1000 g/t.

4.3.4.2 Effects of kerosene dosage and agitation strength on separation efficiency

Fig. 4. 10 shows the relationship between Cu recovery in froth, R_{Cu} (%), and Si recovery in tailing, R_{Si} (%) after agglomeration-flotation (KAX, 200 g/t; agglomeration, 30 min; agitation strength, 1000 rpm and 15000 rpm, kerosene dosage, 15 L kerosene/t sample and 25 L kerosene/t sample). The results showed that with increasing agitation strength and kerosene dosage, Cu recovery increased significantly while Si recovery slightly increased. These results indicate that the separation efficiency, η (%), increased with increasing agitation strength and kerosene dosage. The highest separation efficiency was obtained under the conditions of 200 g/t KAX, 25L kerosene/t sample and 15000 rpm agitation strength.

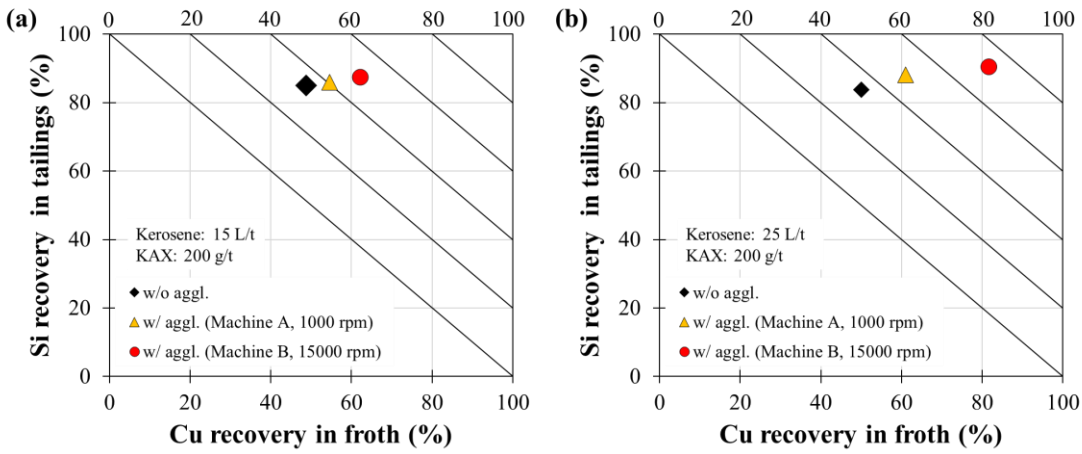

Fig. 4.10. Relationship between Cu recovery in froth, R_{Cu} (%), and Si recovery in tailing, R_{Si} (%), of chalcopyrite and quartz mixture with different kerosene dosage:(**a**) 15 L kerosene/t sample and (**b**) 25 L kerosene/t sample.

4.4 Summary

Agglomeration using emulsified oil is an effective method to improve floatability of finely ground chalcopyrite (D_{50}=3.5 μm). Agitation strength, kerosene and KAX dosages are important parameters for overall Cu recovery and flotation separation efficiency. The main findings of this study are summarized as follows:

- Strong agitation strength is important to produce small oil droplets, which increase the number of oil droplets available for higher frequency of collision with fine particles.
- Increasing kerosene dosage is not effective to improve the Cu recovery when low agitation strength is applied while at high agitation strength, Cu recovery is improved. High agitation strength and high dosage of kerosene provide the high Cu recovery.
- Increasing KAX amount is also effective to improve Cu recovery by probably assisting

attachment of small oil droplets to mineral particles of which hydrophobicity increased by the addition of KAX.

- In the agglomeration-flotation of mixed sample containing chalcopyrite and quartz with 1:1 ratio (w/w), Si recovery in froth is low and is not affected by agitation strength, KAX and kerosene dosages while Cu recovery increases with increasing agitation strength, KAX and kerosene dosages, making separation efficiency higher.

This chapter was modified from Hornn et al., (2020) "Agglomeration-Flotation of Finely Ground Chalcopyrite and Quartz: Effects of Agitation Strength during Agglomeration Using Emulsified Oil on Chalcopyrite". Minerals, 10(4), 380.

References

Acar, S., and Somasundaran, P. (1989). Flocculation of sulfides and the role of a complexing agent in it. *International Journal of Mineral Processing*, *27*(1), 111–123. https://doi.org/10.1016/0301-7516(89)90009-4

Ahmadi, R., Khodadadi, D. A., Abdollahy, M., and Fan, M. (2014). Nano-microbubble flotation of fine and ultrafine chalcopyrite particles. *International Journal of Mining Science and Technology*, *24*(4), 559–566. https://doi.org/10.1016/j.ijmst.2014.05.021

Alonso, M. I., Valdés, A. F., Martínez-Tarazona, R. M., and Garcia, A. B. (1999). Coal recovery from coal fines cleaning wastes by agglomeration with vegetable oils: Effects of oil type and concentration. *Fuel*, *78*(7), 753–759. https://doi.org/10.1016/S0016-2361(98)00218-X

Ateşok, G., Boylu, F., and Çelĭk, M. S. (2001). Carrier flotation for desulfurization and deashing of difficult-to-float coals. *Minerals Engineering*, *14*(6), 661–670. https://doi.org/10.1016/S0892-6875(01)00058-9

Bensley, C. N., Swanson, A. R., and Nicol, S. K. (1977). The effect of emulsification on the selective agglomeration of fine coal. *International Journal of Mineral Processing*, *4*(2), 173–184. https://doi.org/10.1016/0301-7516(77)90024-2

Bhaskar Raju, G., and Khangaonkar, P. R. (1982). Electro-flotation of chalcopyrite fines. *International Journal of Mineral Processing*, *9*(2), 133–143. https://doi.org/10.1016/0301-7516(82)90022-9

Feng, D., and Aldrich, C. (1999). Effect of particle size on flotation performance of complex sulphide ores. *Minerals Engineering*, *12*(7), 721–731. https://doi.org/10.1016/S0892-6875(99)00059-X

Finch, J. A. (1995). Column flotation: A selected review— part IV: Novel flotation devices. *Minerals Engineering*, *8*(6), 587–602. https://doi.org/10.1016/0892-6875(95)00023-J

Fuerstenau, M. C., Jameson, G. J., and Yoon, R.-H. (2007). Column Flotation. In *Froth Flotation: A*

Century of Innovation (pp. 681–705). SME.

Hornn, V., Ito, M., Shimada, H., Joen, S., Park, I., Tabelin, C. B., and Hiroyoshi, N. (2019, 13-17). EARTH 2019. *Agglomeration Flotation of Finely Ground Chalcopyrite: Comparison of Model Calculation vs. Experimental Results*. EARTH 2019 THE 15th INTERNATIONAL SYMPOSIUM ON EAST ASIAN RESOURCES RECYCLING TECHNOLOGY, Korea.

House, C. I., and Veal, C. J. (1989). Selective recovery of chalcopyrite by spherical agglomeration. *Minerals Engineering*, *2*(2), 171–184. https://doi.org/10.1016/0892-6875(89)90038-1

Jiangang, F., Kaida, C., Hui, W., Chao, G., and Wei, L. (2012). Recovering molybdenite from ultrafine waste tailings by oil agglomerate flotation. *Minerals Engineering*, *39*, 133–139. https://doi.org/10.1016/j.mineng.2012.07.006

King, R. P. (2001). *Modeling and Simulation of Mineral Processing Systems*. Elsevier.

Li, X., Xu, H., Liu, J., Zhang, J., Li, J., and Gui, Z. (2016). Cyclonic state micro-bubble flotation column in oil-in-water emulsion separation. *Separation and Purification Technology*, *165*, 101–106. https://doi.org/10.1016/j.seppur.2016.01.021

Mandre, N. R., and Panigrahi, D. (1997). Studies on selective flocculation of complex sulphides using cellulose xanthate. *International Journal of Mineral Processing*, *50*(3), 177–186. https://doi.org/10.1016/S0301-7516(97)00013-6

Mehrotra, V. P., Sastry, K. V. S., and Morey, B. W. (1983). Review of oil agglomeration techniques for processing of fine coals. *International Journal of Mineral Processing*, *11*(3), 175–201. https://doi.org/10.1016/0301-7516(83)90025-X

Miettinen, T., Ralston, J., and Fornasiero, D. (2010). The limits of fine particle flotation. *Minerals Engineering*, *23*(5), 420–437. https://doi.org/10.1016/j.mineng.2009.12.006

Mort, P. R. (2005). Scale-up of binder agglomeration processes. *Powder Technology*, *150*(2), 86–103. https://doi.org/10.1016/j.powtec.2004.11.025

Muganda, S., Zanin, M., and Grano, S. R. (2011). Influence of particle size and contact angle on the flotation of chalcopyrite in a laboratory batch flotation cell. *International Journal of Mineral Processing*, *98*(3), 150–162. https://doi.org/10.1016/j.minpro.2010.11.004

Ng, W. S., Sonsie, R., Forbes, E., and Franks, G. V. (2015). Flocculation/flotation of hematite fines with anionic temperature-responsive polymer acting as a selective flocculant and collector. *Minerals Engineering*, *77*, 64–71. https://doi.org/10.1016/j.mineng.2015.02.013

Ralston, J. (1992). The influence of particle size and contact angle in flotation. In J. S. Laskowski (Ed.), *Colloid Chemistry in Mineral Processing* (pp. 203–224). Elsevier.

Rodrigues, R. T., and Rubio, J. (2007). DAF–dissolved air flotation: Potential applications in the mining and mineral processing industry. *International Journal of Mineral Processing*, *82*(1), 1–13. https://doi.org/10.1016/j.minpro.2006.07.019

Rubio, J., Capponi, F., Rodrigues, R. T., and Matiolo, E. (2007). Enhanced flotation of sulfide fines

using the emulsified oil extender technique. *International Journal of Mineral Processing*, *84*(1), 41–50. https://doi.org/10.1016/j.minpro.2007.04.002

Rubio, Jorge, and Hoberg, H. (1993). The process of separation of fine mineral particles by flotation with hydrophobic polymeric carrier. *International Journal of Mineral Processing*, *37*(1), 109–122. https://doi.org/10.1016/0301-7516(93)90008-X

Sahinoglu, E., and Uslu, T. (2013). Use of ultrasonic emulsification in oil agglomeration for coal cleaning. *Fuel*, *113*, 719–725. https://doi.org/10.1016/j.fuel.2013.06.046

Song, S., Lopez-Valdivieso, A., Reyes-Bahena, J. L., and Lara-Valenzuela, C. (2001). Floc flotation of galena and sphalerite fines. *Minerals Engineering*, *14*(1), 87–98. https://doi.org/10.1016/S0892-6875(00)00162-X

Tao, D., Yu, S., Zhou, X., Honaker, R., and Parekh, B. (2008). Picobubble column flotation of fine coal. *International Journal of Coal Preparation and Utilization*, *28*(1), 1–14.

Trahar, W. J., and Warren, L. J. (1976). The flotability of very fine particles—A review. *International Journal of Mineral Processing*, *3*(2), 103–131.

van Netten, K., Moreno-Atanasio, R., and Galvin, K. P. (2014). Fine Particle Beneficiation through Selective Agglomeration with an Emulsion Binder. *Industrial and Engineering Chemistry Research*, *53*(40), 15747–15754. https://doi.org/10.1021/ie5027502

van Netten, K., Moreno-Atanasio, R., and Galvin, K. P. (2016). Selective agglomeration of fine coal using a water-in-oil emulsion. *Chemical Engineering Research and Design*, *110*, 54–61. https://doi.org/10.1016/j.cherd.2016.02.029

Warren, L. J. (1975). Shear-flocculation of ultrafine scheelite in sodium oleate solutions. *Journal of Colloid and Interface Science*, *50*(2), 307–318. https://doi.org/10.1016/0021-9797(75)90234-9

Waters, K. E., Hadler, K., and Cilliers, J. J. (2008). The flotation of fine particles using charged microbubbles. *Minerals Engineering*, *21*(12–14), 918–923. https://doi.org/10.1016/j.mineng.2008.04.011

Yoon, R.-H. (1993). Microbubble flotation. *Minerals Engineering*, *6*(6), 619–630. https://doi.org/10.1016/0892-6875(93)90116-5

CHAPTER 5: AGGLOMERATION-FLOTATION USING EMULSIFIED OIL STABILIZED BY EMULSIFIERS

5.1 Introduction

In the previous chapter, emulsified oil was used, however, strong agitation strength is required to produce small oil droplets, which increase the number of oil droplets available for higher frequency of collision with fine particles. Moreover, emulsified oil should be added to agglomeration vessel immediately because emulsified oil is unstable. In commercial plant, stability of emulsified oil is important to keep small droplets size for oil agglomeration. This strong agitation during agglomeration requires high energy consumptions, which make the process costly, so it is not easily integrated into the actual flotation circuits.

The emulsifiers can produce small size of oil droplets and stabilize an emulsified oil (Stang et al., 1994). To the best of our knowledge, however, agglomeration-flotation using emulsified oil stabilized by emulsifiers on finely ground chalcopyrite has never been studied. In this chapter, the effects of emulsified oil containing various types of emulsifiers on agglomeration and flotation of finely ground chalcopyrite were investigated.

5.2 Materials and methods

5.2.1 Materials

Chalcopyrite and quartz samples were prepared by identical way as describe in chapter 4.

Potassium amyl xanthate (KAX) (Tokyo Chemical Industry Co., Ltd., Japan), Kerosene (Wako Pure Chemical Industries, Ltd., Japan), Methyl Isobutyl Carbinol (MIBC) (Tokyo Chemical Industry Co., Ltd., Japan), Sodium Dodecyl Sulfate (SDS) (Tokyo Chemical Industry Co., Ltd., Japan), Dodecyl Amine Acetate (DAA) (Tokyo Chemical Industry Co., Ltd., Japan), and Polysorbate 20 (Tween20) (Tokyo Chemical Industry Co., Ltd., Japan) were used in this study. Calcium chloride (Tokyo Chemical Industry Co., Ltd., Japan) was used for study the effects of Ca^{2+} ions. Artificial saline water was used to study the effects of seawater on agglomeration-flotation of finely ground chalcopyrite using emulsified oil stabilized by emulsifiers.

5.2.2 Preparation of emulsified oil with emulsifiers

Anionic (SDS, KAX), cationic (DAA) and non-ionic (Tween 20) emulsifiers were used as emulsifying reagents. 10 mL kerosene was mixed with 40 mL of deionized (DI) water and then 0.1 g of emulsifiers (SDS, KAX, DAA or Tween 20) was added (i.e., concentration of surfactants, 2000 ppm). Then emulsification of the mixture was carried out before agglomeration using an ultrasonic homogenizer (ULTRA-TURRAX, IKA, Germany) for 60 seconds. After emulsification, oil droplet size was

analyzed by laser diffraction sizer.

5.2.3 Stability tests of emulsified oil

Stability tests of emulsified oil containing different emulsifiers were carried out to evaluate the stability of the suspensions (Latreille and Paquin, 1990). The emulsified oil after emulsification was equilibrated for 5 mins until the bubble foams disappear. Then, 50 mL of emulsified oil was centrifuged at 350×g for 20 mins. The volume ratio of oil and emulsion layer were calculated by measuring the thickness of oil layer

5.2.4 KAX conditioning and agglomeration

This process consists of KAX conditioning, agglomeration and flotation, and this process is divided into two ways depending on the agitation speed during agglomeration.

<Agitation speed of agglomeration process: 1000 rpm>

i. KAX conditioning: before agglomeration, 20 g of sample (finely ground chalcopyrite sample, D_{50}= 3.5 μm) was suspended in 400 mL of distilled water (w/ and w/o 400 ppm Ca^{2+}), then the suspension was conditioned with the surface modifier, KAX (200 g/t) for 5 mins at 1000 rpm in the flotation cell (FT-1000, Heiko, Japan).

ii. Agglomeration: after conditioning, emulsified oil (15 L kerosene/t sample, with and without emulsifiers) was added to the suspension, and agitation was carried out at 1000 rpm for 30 mins in the flotation cell.

<Agitation speed of agglomeration process: 15000 rpm>

i. **KAX conditioning**: before agglomeration, 20 g of sample (finely ground chalcopyrite sample, D50= 3.5 μm) was suspended in 400 mL of distilled water, then the suspension was conditioned with the surface modifier, KAX (200 g/t) for 5 mins at 1000 rpm in the flotation cell.

ii. Agglomeration: after conditioning, the suspension was transferred to an agglomeration vessel (high speed mixer with a s-shape impeller, SPB-600J, Cuisinart, USA; fix rotation speed of 15000 rpm), and emulsified oil (15 L kerosene/t sample, with and without emulsifiers was then added and agitation was carried out for 30 mins. Suspension after agglomeration was transferred to a 500 mL flotation cell. Emulsified oil with emulsifiers after emulsification were let sit for 5 mins before agglomeration process to calm down the suspension containing bubble foams. When emulsified oil without surfactant was used it was added immediately before agglomeration because stability of the suspension was bad. After agglomeration, particle size distribution was measured by laser diffraction sizer.

5.2.5 Flotation tests

Flotation was carried out using a same procedure as described in chapter.

5.2.6. FT-IR Measurements

The untreated and treated quartz samples with SDS and/or Ca^{2+} were analysed by ATR-FTIR spectroscopy (FT/IR-6200 HFV and ATR Pro One attachment equipped with a diamond prism, Jasco Analytical Instruments, Japan) to check whether SDS is adsorbed on its surface or not. Suspension containing quartz w/ and w/o 0.001 M of Ca^{2+} were prepared. The suspensions were then conditioned with 1000 ppm of SDS for 15 min in a beaker with magnetic stirrer. Afterwards, the suspension was filtrated, and the residue was dried in the vacuum oven at 40°C for 24 hours. The residues were then analyzed by ATR-FTIR spectroscopy (FT/IR-6200 HFV and ATR Pro One attachment equipped with a diamond prism, Jasco Analytical Instruments, Japan).

5.3 Results and discussion

5.3.1 Effects of emulsifiers on oil droplets size and stability of emulsified oil

Anionic emulsifiers (SDS, KAX), cationic emulsifiers (DAA) and non-ionic emulsifiers (Tween 20) were used as emulsifying agents for preparation of emulsified oil. These emulsifiers were chosen to represent three main types of flotation collector that have great potential to be used as emulsifying agents. Fig. 5.1 shows the size distribution of oil droplets with and without addition of emulsifiers. The results showed that mode size with emulsifiers showed smaller value rather than that without emulsifiers because the emulsifiers can reduce the interfacial tension, thus facilitating the disruption of droplets (Stang et al., 1994). In the chapter 4, emulsified oil was added to agglomeration vessel immediately because emulsified oil without emulsifiers was unstable. In commercial plant, stability of emulsified oil is important to keep small droplets size for oil agglomeration. To check the stability of the suspensions, stability tests were carried out. The volume ratio of oil and emulsion layers are shown in Fig. 5.2. In this test, centrifugation was applied to accelerate coalescence of oil droplets and their moving speed towards the center of centrifugal machine because the thickness of oil layer relies on ease of coalescence and oil droplet size. The volume of oil layer after centrifugation were smaller when emulsifiers were present, indicating that emulsifiers are effective to stabilize the oil droplets and sustain the stability of emulsified oil. Chen and Tao (2005) reported that the stability of an emulsion is defined as the resistance by the dispersed oil droplets against coalescence, and the emulsifying agent can form a thin interfacial film between the two liquids and maintain the emulsion by minimizing the contact, coalescence and aggregation of the internal dispersed phase.

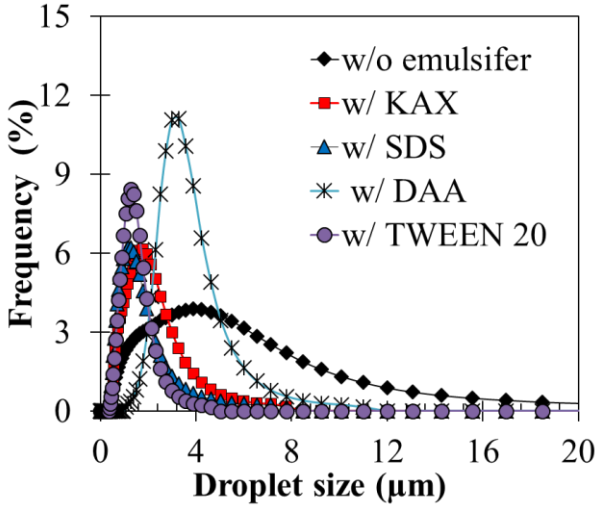

Fig. 5.1. Size distribution of oil droplets after emulsification with and without addition of emulsifiers.

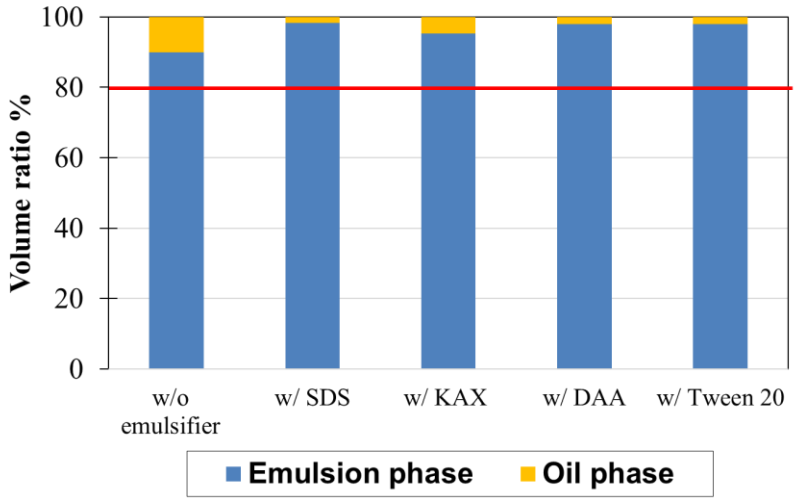

Fig. 5.2. Volume ratio of oil and emulsion layers with and without emulsifiers (after emulsification and centrifugation). Note that the red line indicates volume ratio without emulsification (80% water, 20% oil).

5.3.2 Effects of emulsifiers on agglomeration

In the previous section, SDS, KAX, DAA and Tween 20 were effective to reduce the size of oil droplets and sustain the stability of emulsified oil. The effects of theses emulsifiers on agglomeration of chalcopyrite were investigated. Agglomeration consisting two stages: (1) conditioning in the flotation cell with 200 g/t of KAX; (2) agglomeration using emulsified oil containing 2000 ppm of emulsifiers were carried out (15 L kerosene /t). Fig. 5. 3 shows apparent particle size distribution after

agglomeration (1000 or 15000 rpm for 30 mins). The results showed that when SDS, KAX, and DAA were used, mode size of agglomerate showed larger size rather than that without emulsifiers even high speed (15000 rpm) of agitation. As shown in Fig. 5. 1, droplets size of emulsified oil containing emulsifiers is relatively smaller than that without emulsifiers. When the size of oil droplets become smaller, the number of droplets in the agitator increases. Because frequency of collision of the oil droplets and particles in agglomeration system is proportional to the number of oil droplets, it is reasonable to assume that the number of oil droplets attached on particle surface, induced by the collision of oil droplet and particle, became larger resulting bigger agglomerate size when emulsified oil containing emulsifiers were used.

When Tween 20 was used, mode side of agglomerates showed similar size with that without emulsifiers. Agglomeration kinetic and agglomerate size are mainly determined by (1) particle-particle collision, (2) particle-particle attraction, and (3) decomposition of agglomerate (Hornn et al., 2020). As shown in Fig. 5. 2, size of droplets with Tween 20 were similar with those with other emulsifiers, indicating that probability of collision between particles and oil droplets may be similar but the probability of attraction of particles and oil droplets containing Tween 20 may be lower than that with other emulsifiers.

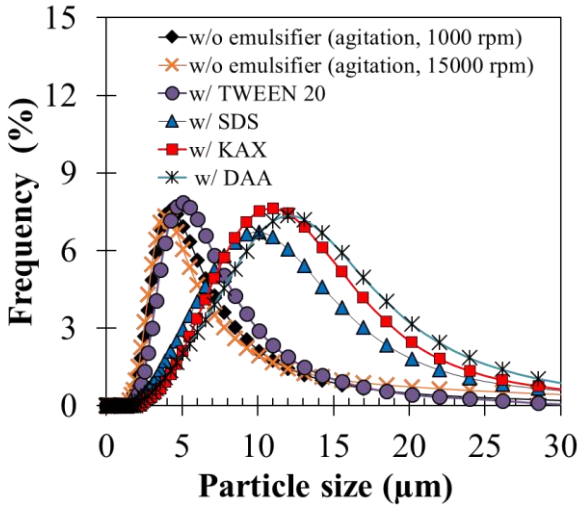

Fig. 5.3 Size distribution after agglomeration (agglomeration conditions: 30 mins; 1000 rpm with emulsifiers, 1000 and 15000 rpm without emulsifiers).

5.3.3 Effects of emulsifiers on flotation

In this flotation test, agglomeration using emulsified oil with and without emulsifiers was carried out and flotation of the agglomerates was conducted. Fig. 5.4 shows the Cu recovery with time (agglomeration conditions: 30 mins; 1000 rpm with emulsifiers, 1000 and 15000 rpm without emulsifiers). In the case of without emulsifiers, Cu recovery with agglomeration using high agitation

strength (15000 rpm) was higher than that with low agitation strength (1000 rpm) indicating that high agitation strength is required for agglomeration-flotation without emulsifiers due to the instability of emulsified oil.

In the case of agglomeration-flotation with Tween 20, Cu recovery showed similar trend with that of without emulsifiers. This result is in-line with the result of size distribution of agglomerate; that is, size of agglomerate using Tween 20 is almost the same as the one without emulsifier.

In the case of agglomeration-flotation with emulsifiers of SDS, DAA and KAX, Cu recovery with agglomeration using these emulsifiers was higher than that with agglomeration but without emulsifiers even high agitation strength (15000 rpm) was applied during agglomeration, indicating that low agitation strength (1000 rpm) is enough for agglomeration-flotation with emulsifiers because high stability of emulsified oil and small droplets size results in bigger agglomerate. This means that when emulsifiers are used, special equipment with higher agitation strength is not required and the process could be easily integrated into existing flotation circuits.

Fig. 5.5 shows the Cu recovery of agglomerate with SDS (agglomeration time: 15 and 30 mins) and the results showed that there was no significant difference of Cu recovery, indicating that agglomeration for 15 mins was enough to achieve high Cu recovery. In other words, the utilization of emulsifiers can shorten agglomeration time.

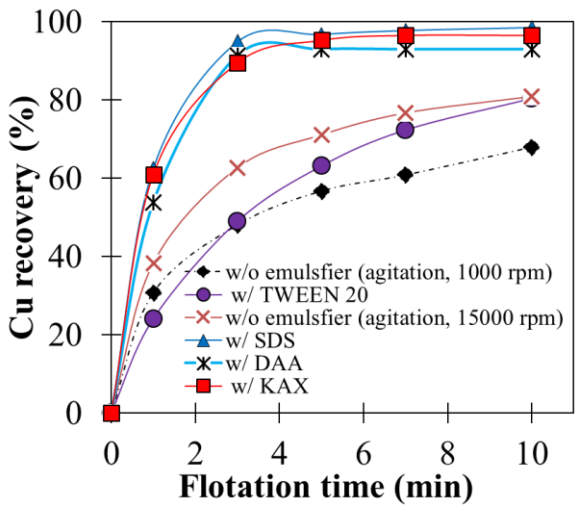

Fig. 5.4. Cu recovery with time (agglomeration conditions: 30 mins; 1000 rpm with surfactants, 1000 and 15000 rpm without emulsifiers).

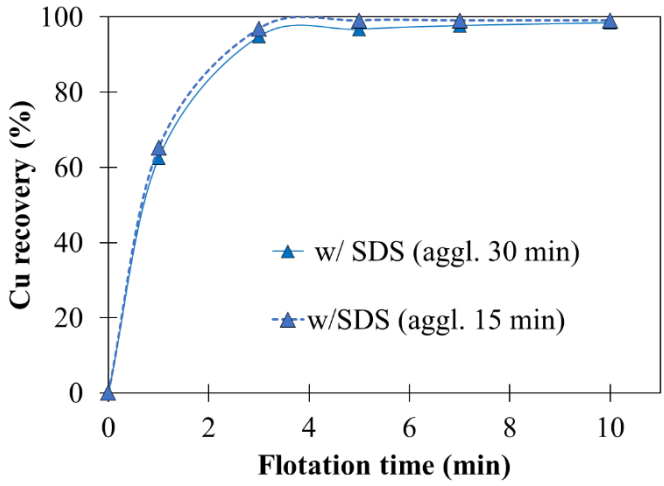

Fig. 5.5. Cu recovery of agglomerate with SDS (agglomeration time: 15 and 30 mins).

5.3.4. Effects of co-existing minerals (quartz) on agglomeration-flotation of chalcopyrite and quartz

Agglomeration-flotation using emulsified oil stabilized by anionic emulsifiers (SDS, KAX) were investigated using a mixture of 10 g of chalcopyrite and 10 g of quartz. Figs. 5.6 (a) and (b) showed Cu recovery and Si recovery after agglomeration-flotation using emulsified oil stabilized by emulsifiers (KAX, SDS). Cu recovery rate with emulsifiers (either KAX or SDS) was higher than that without emulsifier; however, Si recovery rate with KAX or SDS was not increased comparing to that of without emulsifiers addition. These results indicated that the emulsifiers did not interact with quartz, and Cu recovery and separation efficiency were not affected by the co-existence of quartz during agglomeration-flotation.

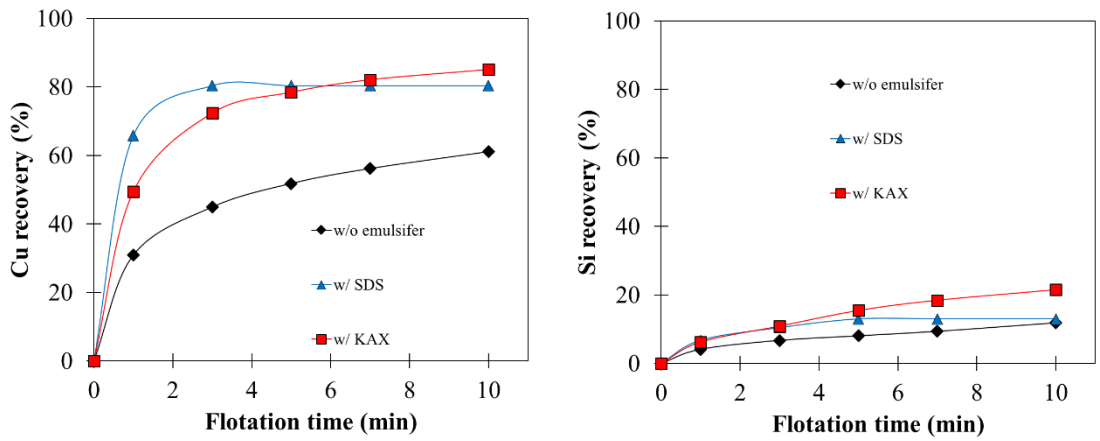

Fig. 5 .6 (a) Cu recovery and (b) Si recovery of agglomeration-flotation of chalcopyrite and quartz w and w/ emulsifiers.

5.3.5 Effects of calcium ions on the agglomeration-flotation

$CaCO_3$ is commonly used as pH adjuster in industrial-scale flotation circuits for sulfide minerals and significant amounts of Ca^{2+} present in the flotation solution. In addition, seawater containing high concentration of Ca^{2+} (about 400 ppm) is required to be used for the beneficiation of mineral deposits located in semi-arid areas (e.g., Chile) due to the shortage of fresh water. This means that significant amount of Ca^{2+} would be presented in the flotation using $CaCO_3$ and/or seawater, so the effects of Ca^{2+} on the agglomeration-flotation of finely ground chalcopyrite using emulsified oil stabilized by anionic emulsifiers (SDS or KAX) were investigated.

5.3.5.1 Single-mineral system (chalcopyrite)

The effects of coexisting Ca^{2+} on agglomeration-flotation using SDS or KAX as emulsifier were carried out w/ and w/o 400 ppm of Ca^{2+}. As shown in Fig. 5.7, the presence of Ca^{2+} have no significant effect on Cu recovery, indicating that when only chalcopyrite presents (single-mineral system), the agglomeration-flotation of chalcopyrite using SDS and KAX as emulsifiers was not affected by Ca^{2+}.

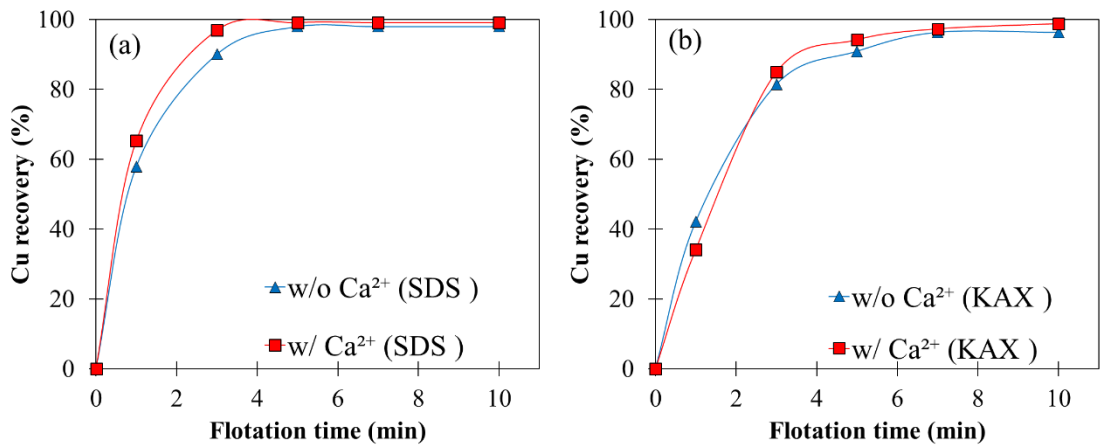

Fig. 5.7. Effects of 400 ppm Ca^{2+} on the agglomeration-flotation of finely ground chalcopyrite using (a) SDS or (b) KAX as emulsifiers to stabilize oil droplet (collector: KAX).

5.3.5.2 Mixed minerals system (chalcopyrite and quartz)

Agglomeration-flotation of a mixture of 10 g of chalcopyrite and 10 g of quartz was carried out with SDS or KAX as emulsifier in the presence and absence of 400 ppm of Ca^{2+}. As shown in Fig. 5.8, when SDS was used as emulsifier, Cu recovery rate with Ca^{2+} was lower than that without Ca^{2+}. On

the other hand, when KAX was used as emulsifier, Cu recovery rate with Ca^{2+} was similar to that without Ca^{2+}. These results suggest that in the presence of Ca^{2+}, Cu recovery rate was decreased when SDS was used as an emulsifier, while KAX works well as the emulsifier regardless of the presences of Ca^{2+}. Thus, effects of quartz on the size distribution of oil droplets prepared with SDS as emulsifier was measured in the presence of 400 ppm of Ca^{2+} (Fig. 5.9).

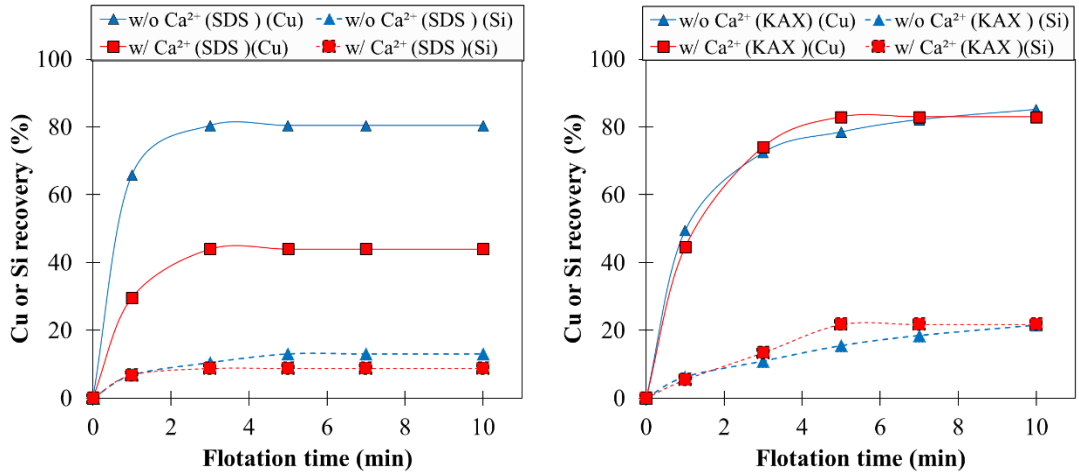

Fig. 5.8. Effects of 400 ppm Ca^{2+}on the agglomeration-flotation of $CuFeS_2$ and SiO_2 mixture using SDS or KAX as emulsifier (Collector: KAX).

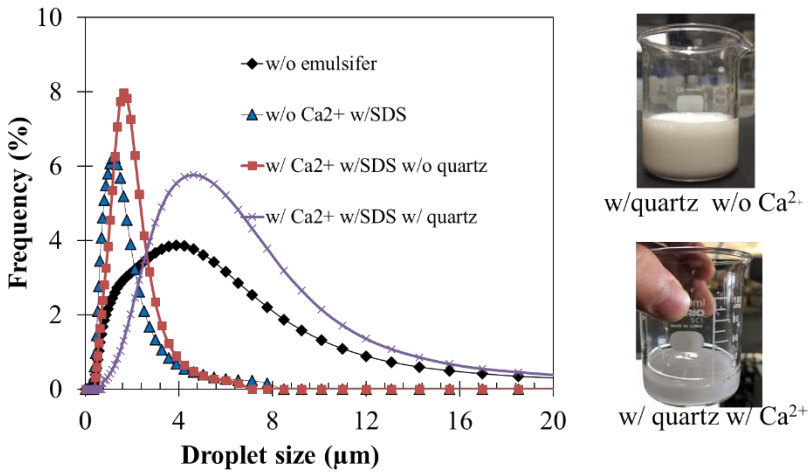

Fig. 5.9. Effects of quartz on the size-distribution of oil droplets in the presence of 400 ppm Ca^{2+} with or without emulsifier (SDS).

As described in the previous section, mode size of oil droplets with SDS is smaller than those without addition of SDS resulting in high Cu recovery rate. In the presence of 400 ppm of Ca^{2+}, the mode size of oil droplets with SDS was slightly increased, so the Cu recovery rate was still high. When quartz was added together with Ca^{2+}, mode size of oil droplets using SDS as emulsifier became larger

than that without addition of quartz.

It was also observed that in the presence of quartz and Ca^{2+}, clear oil layer on top of kerosene/water emulsion with SDS as emulsifier was observed (Fig. 5.9), suggesting that coalescence of kerosene droplets occurred causing the increase in oil droplets size.

It has been well known that surface potential of quartz shows negative at pH greater than 2, so positively charged Ca^{2+} can be adsorbed on its surface by the electrostatic attraction. Meanwhile, SDS shows a strong chemical affinity with Ca^{2+}(Sammalkorpi et al., 2009), so in the presence of quartz, SDS may be chemically combined with Ca^{2+} adsorbed on quartz surface, causing a decrease in the amount of SDS remained in the interface of oil and water. This may be the reason of the increase in the size of oil droplets with SDS in the presence of Ca^{2+} and quartz and this may be the reason of the suppression in Cu recovery rate. Because chemical affinity between Ca^{2+} and KAX is very weak, KAX would not combine with Ca^{2+} adsorbed on quartz, resulting in small oil droplets and high Cu recovery rate.

To confirm whether SDS is adsorbed on the surface of quartz when Ca^{2+} co-existed, three types of samples—i) quartz, ii) quartz w/ SDS, and iii) quartz w/ SDS and Ca^{2+}—were prepared and analyzed by FT-IR. As shown in Fig. 5.10, IR spectrum of quartz with SDS and Ca^{2+} showed the additional peaks at 866, 1250, 2854, and 2927 cm^{-1}, which were not observed in other spectra. According to Zeng et al. (2017), the IR signatures of SDS are as follow: CH bonds in the CH_2− and CH_3 groups for the alkyl chain (2921 and 2848 cm^{-1}). asymmetric stretching and symmetric stretching of S=O (1219 and 1080 cm^{-1}) and C−O−S stretching (830 cm^{-1}). These results indicate that SDS can absorb onto quartz surface in the presence of Ca^{2+}.

When Ca^{2+} is present with co-existing minerals like quartz, SDS cannot be used as an emulsifier because of the adsorption of SDS on to Ca^{2+} site bound to quartz, resulting in the reduction of SDS amount available for emulsifying the oil droplets. As a result, oil droplets size becomes bigger, and the efficiency of agglomeration-flotation of finely ground chalcopyrite decreased.

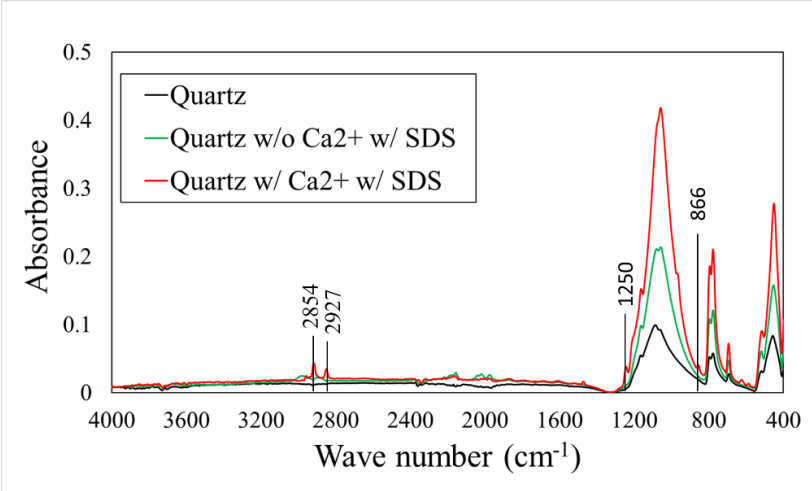

Fig. 5.10. FT-IR Spectrum of i) quartz, ii) quartz w/ SDS, and iii) quartz w/ SDS and Ca^{2+}.

5. 4 Summary

The following conclusions can be drawn from the agglomeration-flotation study using emulsified oil with emulsifiers:

- Addition of emulsifiers (e.g., SDS, KAX, DAA and Tween 20) can reduce the size of oil droplets and sustain the stability of emulsified oil.
- Addition of emulsifiers to emulsified oil can contribute to the bigger size of agglomerate compared to the result without addition of emulsifier.
- Addition of emulsifiers such as SDS can obtain high Cu recovery even low agitation strength and shorter agglomeration time.
- When emulsified oil with emulsifiers is used, special equipment with higher agitation strength during agglomeration is not required, and thus the process could be easily integrated into existing flotation circuits.
- When Ca^{2+} is present with co-existing minerals like quartz, SDS cannot be used as an emulsifier because of the adsorption of SDS on to Ca^{2+} site bound to quartz, resulting in the reduction of SDS amount available for emulsifying the oil droplets. As a result, oil droplets size becomes bigger, and the efficiency of agglomeration-flotation of finely ground chalcopyrite decreased. Controlling of oil droplets size is essential for agglomeration-flotation process.

This chapter was modified from Hornn et al., (2020) "Agglomeration–Flotation of Finely Ground Chalcopyrite Using Emulsified Oil Stabilized by Emulsifiers: Implications for Porphyry Copper Ore Flotation". Metals, 10(7), 912.

References

Alonso, M. I., Valdés, A. F., Martínez-Tarazona, R. M., and Garcia, A. B. (1999). Coal recovery from coal fines cleaning wastes by agglomeration with vegetable oils: Effects of oil type and concentration. *Fuel*, *78*(7), 753–759. https://doi.org/10.1016/S0016-2361(98)00218-X

Bensley, C. N., Swanson, A. R., and Nicol, S. K. (1977). The effect of emulsification on the selective agglomeration of fine coal. *International Journal of Mineral Processing*, *4*(2), 173–184. https://doi.org/10.1016/0301-7516(77)90024-2

Bhaskar Raju, G., and Khangaonkar, P. R. (1982). Electro-flotation of chalcopyrite fines. *International Journal of Mineral Processing*, *9*(2), 133–143. https://doi.org/10.1016/0301-7516(82)90022-9

Chen, G., and Tao, D. (2005). An experimental study of stability of oil–water emulsion. *Fuel Processing Technology*, *86*(5), 499–508. https://doi.org/10.1016/j.fuproc.2004.03.010

Dai, Z., Fornasiero, D., and Ralston, J. (2000). Particle–bubble collision models—A review. *Advances in Colloid and Interface Science*, *85*(2–3), 231–256. https://doi.org/10.1016/S0001-8686(99)00030-5

Finch, J. A. (1995). Column flotation: A selected review— part IV: Novel flotation devices. *Minerals Engineering*, *8*(6), 587–602. https://doi.org/10.1016/0892-6875(95)00023-J

Hornn, V., Ito, M., Shimada, H., Tabelin, C. B., Jeon, S., Park, I., and Hiroyoshi, N. (2020). Agglomeration-Flotation of Finely Ground Chalcopyrite and Quartz: Effects of Agitation Strength during Agglomeration Using Emulsified Oil on Chalcopyrite. *Minerals*, *10*(4), 380. https://doi.org/10.3390/min10040380

Jiangang, F., Kaida, C., Hui, W., Chao, G., and Wei, L. (2012). Recovering molybdenite from ultrafine waste tailings by oil agglomerate flotation. *Minerals Engineering*, *39*, 133–139. https://doi.org/10.1016/j.mineng.2012.07.006

Laskowski, J. S., Liu, Q., and Bolin, N. J. (1991). Flotation of sulphide minerals 1990 Polysaccharides in flotation of sulphides. Part I. Adsorption of polysaccharides onto mineral surfaces. *International Journal of Mineral Processing*, *33*(1), 223–234. https://doi.org/10.1016/0301-7516(91)90054-M

Latreille, B., and Paquin, P. (1990). Evaluation of Emulsion Stability by Centrifugation with Conductivity Measurements. *Journal of Food Science*, *55*(6), 1666–1668. https://doi.org/10.1111/j.1365-2621.1990.tb03595.x

Miettinen, T., Ralston, J., and Fornasiero, D. (2010). The limits of fine particle flotation. *Minerals Engineering*, *23*(5), 420–437. https://doi.org/10.1016/j.mineng.2009.12.006

Rodrigues, R. T., and Rubio, J. (2007). DAF–dissolved air flotation: Potential applications in the mining and mineral processing industry. *International Journal of Mineral Processing*, *82*(1), 1–13. https://doi.org/10.1016/j.minpro.2006.07.019

Rubio, J., and Hoberg, H. (1993). The process of separation of fine mineral particles by flotation with hydrophobic polymeric carrier. *International Journal of Mineral Processing*, *37*(1), 109–122. https://doi.org/10.1016/0301-7516(93)90008-X

Sahinoglu, E., and Uslu, T. (2013). Use of ultrasonic emulsification in oil agglomeration for coal cleaning. *Fuel*, *113*, 719–725. https://doi.org/10.1016/j.fuel.2013.06.046

Sammalkorpi, M., Karttunen, M., and Haataja, M. (2009). Ionic Surfactant Aggregates in Saline Solutions: Sodium Dodecyl Sulfate (SDS) in the Presence of Excess Sodium Chloride (NaCl) or Calcium Chloride (CaCl2). *The Journal of Physical Chemistry B, 113*(17), 5863–5870. https://doi.org/10.1021/jp901228v

Slaghuis, J. H., and Ferreira, L. C. (1987). Selective spherical agglomeration of coal. *Fuel*, *66*(10), 1427–1430. https://doi.org/10.1016/0016-2361(87)90191-8

Song, S., Lopez-Valdivieso, A., Reyes-Bahena, J. L., and Lara-Valenzuela, C. (2001). Floc flotation of galena and sphalerite fines. *Minerals Engineering*, *14*(1), 87–98. https://doi.org/10.1016/S0892-6875(00)00162-X

Sresty, G. C., and Somasundaran, P. (1980). Selective flocculation of synthetic mineral mixtures using modified polymers. *International Journal of Mineral Processing*, *6*(4), 303–320. https://doi.org/10.1016/0301-7516(80)90027-7

Stang, M., Karbstein, H., and Schubert, H. (1994). Adsorption kinetics of emulsifiers at oil—Water interfaces and their effect on mechanical emulsification. *Chemical Engineering and Processing: Process Intensification*, *33*(5), 307–311. https://doi.org/10.1016/0255-2701(94)02000-0

Trahar, W. J. (1976). The selective flotation of galena from sphalerite with special reference to the effects of particle size. *International Journal of Mineral Processing*, *3*(2), 151–166. https://doi.org/10.1016/0301-7516(76)90031-4

Trahar, W. J., and Warren, L. J. (1976). The flotability of very fine particles—A review. *International Journal of Mineral Processing*, *3*(2), 103–131.

van Netten, K., Moreno-Atanasio, R., and Galvin, K. P. (2014). Fine Particle Beneficiation through Selective Agglomeration with an Emulsion Binder. *Industrial and Engineering Chemistry Research*, *53*(40), 15747–15754. https://doi.org/10.1021/ie5027502

Warren, L. J. (1975). Shear-flocculation of ultrafine scheelite in sodium oleate solutions. *Journal of Colloid and Interface Science*, *50*(2), 307–318. https://doi.org/10.1016/0021-9797(75)90234-9

Yoon, R.-H. (1993). Microbubble flotation. *Minerals Engineering*, *6*(6), 619–630. https://doi.org/10.1016/0892-6875(93)90116-5

Zeng, X., Xu, L., Tian, J., Yin, W., Yang, Y., and Deng, W. (2017). Effect of a CA depressant on flotation separation of celestite from fluorite and calcite using SDS as a collector. *Minerals*

Engineering, *111*, 201–208. https://doi.org/10.1016/j.mineng.2017.06.019

CHAPTER 6: GENERAL CONCLUSION

Chalcopyrite is the main source of copper worldwide and flotation is often used to concentrate chalcopyrite and remove most of associated gangue minerals prior to smelting processes. In mechanical flotation cells, collisions between fine particles and rising bubbles become poor because of their small mass and low momentum. Because of this, fine particles do not easily attach onto bubbles that leads to substantial losses of selected valuable minerals. In this study, oil agglomeration was applied to increase the size of finely ground chalcopyrite (D_{50}=3.5 μm) before flotation. It was found that oil agglomeration is an effective method for recovering finely ground chalcopyrite. Here are the summaries of the study:

Chapter 1 described the statement of the problem, background of fine particle problems in flotation and objectives of this study.

Chapter 2 reviewed technologies to improve fine recovery in flotation, including microbubble flotation, column flotation, shear flocculation, carrier flotation, oil agglomeration, and polymer flocculation.

Chapter 3 investigated the agglomeration-flotation behavior of finely ground chalcopyrite experimentally using KAX as surface modifier and kerosene as "bridging" liquid. Oil-agglomeration before flotation increased the apparent size of chalcopyrite particles and improved the Cu recovery rate. Flotation rate calculated by first-order kinetic model fitted well with the experimental results of un-agglomerated chalcopyrite; however, it did not fit the experimental results of agglomeration-flotation because agglomeration occurred in the flotation cell after oil agglomeration. A new approach to calculate the Cu recovery rate of agglomerated chalcopyrite was proposed.

In Chapter 4, effects of agitation strength during agglomeration, dosage of KAX as surface modifier and dosage of oil as bridging liquid on Cu recovery and separation efficiency of chalcopyrite and quartz were investigated. Increasing of agitation strength, kerosene oil and KAX dosages improved Cu recovery rate and separation efficiency. Strong agitation strength could produce small oil droplets, which increase the number of oil droplets available for higher frequency of collision with fine particles.

In Chapter 5, agglomeration-flotation using emulsified oil with emulsifiers were investigated. Addition of emulsifiers (i.e., SDS, KAX, DAA and Tween 20) could reduce the size of oil droplets and sustain the stability of emulsified oil and these contributed to the bigger size of agglomerate compared to the result without addition of emulsifiers resulting in higher Cu recovery. This means that controlling of oil droplets size is essential for agglomeration-flotation process. When Ca^{2+} is present with co-existing minerals like quartz, however, SDS cannot be used as an emulsifier because of the adsorption of SDS on to Ca^{2+} site bound to quartz, resulting in the reduction of SDS amount available for emulsifying the oil droplets. As a result, oil droplets size becomes bigger, and the efficiency of

agglomeration-flotation of finely ground chalcopyrite decreased. When emulsified oil with emulsifiers is used, special equipment with higher agitation strength during agglomeration is not required, and thus the process could be easily integrated into existing flotation circuits.

Finally, chapter 6 gave the general conclusions of this study.

ACKNOWLEDGMENT

This dissertation become a reality because I have received a great deal of support and assistance. I would like to thank the following people, without whom I would not have been able to complete this research, and without whom I would not have made it through my doctoral degree.

Foremost, I would like to express my deepest appreciation for my supervisor, Assoc. Prof. Mayumi Ito, for her kindness, patience, motivation, and all the support since my master's program until the doctoral program. She gave me a lot of constructive advice to succeed in my research and life. I feel really happy and fortunate to work under your kind guidance.

Beside this, I would like to express my gratitude to Prof. Naoki Hiroyoshi, for his wisdom, knowledge, and advice of this study. Your valuable advice and critical comments for the improvements of my research are gratefully appreciated. I am highly indebted for his kindness and patience for the past five years.

My sincere thanks are extended to Asst. Prof. Ilhwan Park, for his kind suggestion on conducting research and paper-writing. Thank you very much for your time and effort.

I would also express my gratitude for the former Asst. Prof. Carlito Baltazar Tebelin for his kind support and valuable advice for my research, paper writing and life in general.

Special thanks are to Mr. Hiromasa Shimada and Mr. Ryusuke Yamasawa, for their assistance on this research. I would like to say thank you for putting your trust in me and for always helping me in academic and university matters.

Many thanks are extended to all members in Laboratory of Mineral Processing and Resources Engineering, Graduate School of Engineering, Hokkaido University, Japan, and Department of Geo-Resources and Geotechnical Engineering, Institute of Technology of Cambodia, whose friendship and support are beyond a place of study.

I am deeply grateful to the MEXT (Ministry of Education, Culture, Sports, Science and Technology Japan) for awarding me the scholarship to study in Japan. In addition, I would also like to thank Sumitomo Metals and Mining Co., Ltd. for their financial support and advice for my research.

Finally, I am forever grateful to my parent (Mr. Sitha Phouen and Ms. Malis San), and my siblings (Mrs. Thavy Hornn and Mr. Vothea Hornn) who have always supported and encouraged me to do my best in all matters of life.